

DRUG DEVELOPMENT RESEARCH

RESEARCH ARTICLE

Neuroprotective Effect of Empagliflozin/Rivastigmine in Alzheimer's Disease Rat Model: Optimization of Multifaceted Mechanism of Action

Ebtsam S. Abdel-lah^{1,2} D | Nashwa Hamad³ D | Amira F. Taha⁴ | Wafaa H. Mohamed⁵ | Mariam A. Fawy⁶ | Abdelraheim H. Attaai^{7,8} D | Fatma Y. A. Abbas⁹ | Hoda S. Sherkawy¹⁰ | Ahmed Abdelwarith¹¹ | Marwa G. Gamea^{12,13}

¹Department of Pharmacology, Faculty of Veterinary Medicine, Assiut University, Assiut, Egypt | ²Department of Pharmacology, School of Veterinary Medicine, Badr University in Assiut, Naser city, Egypt | ³Department of Pathology, Faculty of Veterinary Medicine, Assiut University, Assiut, Egypt | ⁴Department of Pharmacology and Toxicology, Faculty of Pharmacy, Assiut University, Assiut, Egypt | ⁵Department of Forensic Medicine and Toxicology, Faculty of Veterinary Medicine, Aswan University, Aswan, Egypt | ⁶Department of Zoology, Faculty of Science, South Valley University, Qena, Egypt | ⁷Department of Anatomy and Embryology, Faculty of Veterinary Medicine, Assiut University, Assiut, Egypt | ⁸Department of Anatomy and Histology, School of Veterinary Medicine, Badr University in Assiut, Naser City, Egypt | ⁹Department of Medical Physiology, Faculty of Medicine, Assiut University, Aswan, Egypt | ¹¹Department of Neuropsychiatry, Faculty of Medicine, Aswan University, Assiut, Egypt | ¹²Department of Pharmacology, Faculty of Medicine, Assiut University, Assiut, Egypt | ¹³Basic Medical Science Department, Badr University, Assiut, Egypt

Correspondence: Ebtsam S. Abdel-lah (ebtsam_saber@aun.edu.eg; ebtsam_saber@hotmail.com)

Received: 27 August 2025 | Revised: 1 October 2025 | Accepted: 17 October 2025

Funding: The authors received no specific funding for this work.

Keywords: Alzheimer's disease | empagliflozin | glucose transporters | heavy metal mixtures | rats | rivastigmine | scopolamine

ABSTRACT

This study assessed the neuroprotective potential of empagliflozin (EMPA) as antidiabetic drug on glucose metabolism, comparing it to rivastigmine (RIVA) as standard treatment for Alzheimer's disease (AD), and their combination. Male rats were sorted into five groups. Group I served as the control, while groups II, III, IV, and V received the scopolamine plus heavy metal mixture for AD induction. Groups III and IV were administered RIVA and EMPA, respectively, and group V received both treatments. Cognitive function was evaluated behaviorally. Subsequently, glucose levels, acetylcholinesterase, oxidative stress, and inflammatory markers were assessed. Alongside the brain histopathological changes, the expression of phosphorylated tau protein was assessed. Moreover, glycolytic enzymes and glucose transporters were assessed using PCR analysis. The findings were attributed to a notable suppressive impact of EMPA on lipid peroxidation, acetylcholinesterase, glucose levels, phosphorylated tau protein, pro-inflammatory cytokines, and neuropathological changes, while enhancing antioxidant and interleukin-10 levels. It also improves glucose metabolism. The findings suggest that EMPA may be a viable candidate for future therapeutic exploration in AD, which has a multifaceted mechanism of action encompassing anti-neuroinflammation, antioxidant stress, and enhanced glucose metabolism, as well as decreased acetylcholinesterase activity and phosphorylated tau protein levels. Interestingly, combined treatment showed a superior effect than EMPA alone.

Abbreviations: AChE, acetylcholinesterase; AD, Alzheimer's disease; As, Arsenic; A β , amyloid β ; CAT, catalase; Cd, Cadmium; EMPA, empagliflozin; GLUC, glucose; GLUT1, glucose transporters 1; GLUT3, glucose transporters 3; HIF, hypoxia-inducible factor; HMM, Heavy metal mixture; IL-10, interleukin-10; IL-1 β , Interleukin 1 beta; IL-6, interleukin-6; LDH-A, lactate dehydrogenase; MDA, Malondialehyde; MWM, Morris water maze; NC, normal control; NFT, neurofibrillary tangles; NF- κ B, Nuclear Factor Kappa B; OS, oxidative stress; PA, Passive avoidance; Pb, Lead; PDK-1, pyruvate dehydrogenase kinase 1; RIVA, Rivastigmine; ROS, Reactive oxygen species; SCO, Scopolamine; SGLT-2is, sodium-glucose cotransporter-2 inhibitors; SOD, superoxide dismutase; STL, Step-through latency; TNF- κ C, Tumor necrosis factor- κ C.

© 2025 Wiley Periodicals LLC.

1 | Introduction

Dementia is predominantly caused by Alzheimer's disease (AD), particularly in the elderly population. Age is the primary development risk element of AD. Certain incidences of AD have been documented in individuals aged 40–50, referred to as early-onset AD (Mahaman et al. 2023) and mainly genetic defects cause early-onset AD (Cunnane et al. 2011).

Numerous theories have been posited to elucidate the etiology of Alzheimer's illness, including the aggregation of neuritic extracellular amyloid plaques in the brain. In addition, the hyperphosphorylated microtubule protein tau aggregates in neurofibrillary tangles (NFT) in neurons (Knopman et al. 2021). The notable reduction in cholinergic activity represented one of the initial pathological elements identified in AD (Yadang et al. 2020).

A proposed mechanism by which brain glucose uptake/ metabolism can lead to neurofibrillary degeneration in the AD brain. In the normal brain, tau is changed by both O-GlcNAcylation and phosphorylation, and these two changes maintain equilibrium. Multiple environmental, metabolic, and genetic variables contribute to poor glucose uptake and metabolism in Alzheimer's disease, resulting in reduced intracellular UDP-GlcNAc and tau O-GlcNAcvlation. Due to the negative relationship between O-GlcNAcylation and tau phosphorylation, the reduced tau phosphorylation, or hyperphosphorylation, is made possible by O-GlcNAcylation. In addition to being unable to promote microtubule assembly or stabilize microtubule structures, the aberrant hyperphosphorylation also acts as a poisonous substance that disrupts microtubules and sequesters normal microtubule-associated proteins. Dementia originates from retrograde neurodegeneration caused by the disruption of the microtubule network, which also impairs axonal transport. Additionally, tau's aberrant hyperphosphorylation encourages the formation of neurofibrillary tangles, which leads to neurofibrillary degeneration (Gong et al. 2006; Lanzillotta et al. 2025).

Multiple investigations have established the fact that type 2 diabetes mellitus (T2DM) serves as A contributory element in AD. Conversely, other studies indicate that individuals having AD exhibit an elevated chance of acquiring T2DM (Moreira et al. 2009). T2DM induces considerable and ongoing OS, generates inflammatory cytokines, and leads to macrovascular damage and amyloid deposits. Recent research indicates a notable reduction in memory and cognitive abilities in individuals with T2DM, with a positive correlation observed between its pathogenesis and AD (Alam et al. 2021).

The previously mentioned findings paved the way for exploring the possible neuroprotective effects of various antidiabetic medications. Sodium-glucose transporter 2 inhibitors (SGLT-2i) represent a significant category of antidiabetic medications. Empagliflozin (EMPA), classified as an SGLT2 inhibitor, received FDA approval in 2014 for its use as an antidiabetic agent. Long-term treatment with EMPA in diabetic mice demonstrates a notable preservation of learning and memory, alongside enhancements in cognitive functions. The findings indicate a correlation with decreased levels of OS markers within the brain (Lin et al. 2014). Multiple preclinical models and clinical findings

indicate that EMPA exhibits significant antioxidant, cardioprotective, and neuroprotective effects through enhanced glycemic control and decreased body weight in patients with T2DM (Domínguez et al. 2012; Alhakamy et al. 2024). Recently, EMPA exhibited neuroprotective implications in an experimental Parkinson's disease model throughout the management of inflammation and OS (Ahmed et al. 2022).

In the present investigation, to induce cognitive impairment, a scopolamine and heavy metal mixture (SCO + HMM) was employed. Based on a previous study reported by Assi et al. (Assi et al. 2023), The classic SCO model was strengthened by the integration of HMM to improve its pathological characteristics.

Accordingly, this investigation aimed to explore the neuroprotective benefits of EMPA compared to rivastigmine (RIVA), a conventional standard drug, and their combination against SCO and HMM-induced cognitive impairment in rats. The present investigation focused on the potential effects of EMPA on glucose transport and metabolism, the cholinergic system, OS, and neuroinflammation in AD.

2 | Material and Methods

2.1 | Animals

Forty male adult *Wistar* rats were employed in this study, weighing between 200 and 250 g on average, and were acquired from the Faculty of Veterinary Medicine at Assiut University, Egypt. Rats were accommodated in stainless steel enclosures within an adequately ventilated chamber, maintaining a temperature of $25 \pm 4^{\circ}$ C and a light/dark cycle that lasted for a total of 12 h. The rats were free to get food and water whenever they wanted, and all attempts were undertaken to mitigate the animals' suffering throughout the study period. The ethical committee of the Faculty of Pharmacy at Assiut University, Egypt, approved the study under authorization number 05-2024-028. The US standards for the Care and Use of Laboratory Animals were followed in every step of the experiments.

2.2 | Drugs and Chemicals

Empagliflozin powder was acquired from Jardiance, Boehringer Ingelheim International GmbH, Germany, and dissolved in saline; RIVA and Scopolamine hydrobromide trihydrate were supplied from Sigma Chemical Co., St. Louis, MO, USA, and dissolved in saline. As, Cd and Pb were acquired from BDH Chemicals Ltd (Poole, England).

2.3 | Induction of Alzheimer's Disease

Rat models of AD were established using the method reported in the previous study by Assi et al. (2023). Scopolamine hydrobromide trihydrate, along with a heavy metal mixture, was used to produce cognitive impairment in rats. For 28 days, 4 mg/kg of scopolamine was administered intraperitoneally (I.P.) once daily (Assi et al. 2022). Throughout the experiment, rats were given a

heavy metals mixture (HMM) in their drinking water. 3.80 ppm of As, 0.98 ppm of Cd, and 2.22 ppm of Pb were the components of the HMM (Ashok et al. 2015; Ashok and Rai 2023).

2.4 | Experimental Design

Five groups of eight rats each were created. Group I served as the control, receiving IP injections of saline for 28 days, while groups II, III, IV, and V received a combination of SCO + HMM to induce AD. SCO was injected IP at a dose of 4 mg/kg/day, and HMM was administered in their drinking water for 28 days. Groups III and IV were administered RIVA at a dose of 2 mg/kg/day, P.O. (Yanev et al. 2015), and EMPA at 10 mg/kg/day, P.O. (Borikar et al. 2024), respectively, and group V received a combination of RIVA and EMPA at the same previously mentioned doses.

2.5 | Sample Preparation

Rats were euthanized by employing thiopental sodium anesthesia following behavioral evaluation. Their brains were meticulously excised and rinsed with cold saline. The two hemispheres of each brain were separated, with the left hemisphere designated for histological and immunohistochemical analysis. The remaining brain tissues were concurrently preserved at -80° C for subsequent real-time PCR analysis of GLUT-1, GLUT-3, LDH-A, and PDK-1. The right hemisphere hippocampus of each rat was dissected, dried, weighed, and stored at -80° C. Before testing, the hippocampal samples were combined with PBS (pH 7.4) and centrifuged for 10 min to remove any residual material before conducting ELISA and colorimetric assessments.

2.6 | Behavioral Tests

A series of behavioral paradigms was conducted in the following pattern: y-maze spontaneous alteration, PA, and MWM tests, with the methods elaborated in detail in the supporting materials.

2.6.1 | Y-Maze Spontaneous Alternation Test

This assessment is predicated on the innate inclination of rodents to investigate novel environments and evaluates their short-term spatial learning, memory, and spontaneous alternation. was conducted by the methodology explained by Saad, Samman, and their colleagues (Saad et al. 2018; Samman et al. 2023).

2.6.2 | Passive Avoidance (PA) Test

The PA test is a fear-based assessment tool that is employed in rat models of CNS diseases to assess memory and learning. This technique depends on a combination of environmental conditions, modest foot shock, and disagreeable stimuli. The PA test was conducted using the procedure described by Abdel-Aal et al. (Abdel-Aal et al. 2011).

2.6.3 | Morris Water Maze (MWM)

The MWM test assesses the learning and spatial memory capabilities that are dependent on the hippocampal region. The technique described by (Abdel-lah et al. 2025; Samman et al. 2023) were employed to conduct the MWT.

2.7 | Estimating the Amount of Pro-Inflammatory and Anti-Inflammatory Mediators in the Hippocampus

TNF- α , IL-6, and IL-10 were analyzed using the enzyme-linked immunosorbent assay (ELISA) method, following a methodology based on the rat ELISA kit (Cusabio, Houston, USA), as directed by the manufacturer's outlines.

2.8 | Assessment of OS Markers in the Hippocampus

MDA levels in the hippocampus, a sign of lipid peroxidation, along with superoxide dismutase (SOD) and catalase (CAT), were used to examine how medicine changed the oxidant/antioxidant balance in the brains of diseased rats, possibly acting as a mechanism to enhance memory function. The manufacturer's guidelines were followed to measure the hippocampus MDA level using an MDA ELISA kit (Elabscience, Houston, USA).

The hippocampal level of SOD was evaluated using the Rat SOD ELISA kit (Cusabio, Houston, USA) and the CAT by CAT ELISA kit for rats (MyBiosource, CA, USA) in accordance with the manufacturer's specifications.

2.9 | Determination of Acetylcholinesterase (AChE) Level

An AChE ELISA kit for rats was used to measure the activity of AChE in the hippocampus (Cusabio, Houston, USA) According to the providers' guidelines.

2.10 | Assessment of Hippocampal Glucose (GLUC) Levels

A Colorimetric Assay Kit was used to measure GLUC levels in hippocampal tissue in accordance with the instructions provided by the manufacturer. (GOD-POD) Method (Elabscience, Houston, USA).

2.11 | Real-Time Quantitative Polymerase Chain Reaction Analysis

TRIzol reagent (Invitrogen, USA) was employed to extract total RNA. The spectrophotometric measurement of the extract RNA's concentration and purity was conducted at 260 nm using the Nano Drop System (Thermo Fisher Scientific Inc, USA). Subsequently, the QuantiTect Reverse Transcription Kit

Drug Development Research, 2025 3 of 17

(Qiagen, USA) was employed to reverse-transcribe one microgram of total RNA into single-stranded complementary DNA. Real-time PCR was performed using Roter-Gene Q (Qiagen, USA). To amplify C-DNA amplicons, Thermo Scientific Maxima SYBR Green/Fluorescein qPCR Master Mix (2X) with gene-specific primers, as shown in Supporting Information S1: Table 1, was employed following the manufacturer's protocol. The mRNAs of the GLUT-1, GLUT-3, LDH-A, and PDK-1 genes were normalized against glyceraldehyde 3-phosphate dehydrogenase (GAPDH), which served as the housekeeping gene. Each sample underwent real-time PCR in duplicate, and the average of the duplicates was utilized for further investigation. The 2-\text{\text{-}\text{-}\text{\text{-}\text{\text{-}\text{-}\text{\text{-}\text{\text{-}\text{-}\text{\text{-}\text{\text{-}\text{\text{-}\text{-}\text{\text{-}\text{-}\text{\text{-}\text{\text{-}\text{\text{-}\text{-}\text{\text{-}\text{\text{-}\text{-}\text{-}\text{\text{-}\text{-}\text{\text{-}\text{-}\text{\text{-}\text{\text{-}\text{-}\text{-}\text{\text{-}\text{\text{-}\text{-}\text{\text{-}\text{\text{-}\text{-}\text{\text{-}\text{-}\text{-}\text{-}\text{\text{-}\text{\text{-}\text{-}\text{-}\text{-}\text{-}\text{\text{-}\text{-}\text{\text{-}\text{-}\text{-}\text{-}\text{-}\text{-}\text{\text{-}\text{-}\text{-}\text{-}\text{-}\text{-}\text{-}\text{-}\text{\text{-}\text{-}\text{-}\text{-}\text{-}\text{-}\text{-}\text{-}\text{-}\text{-}\text{-}\text{-}\tex

2.12 | Histopathological Examination

The brain tissue specimens of rats from the control and other groups were obtained and fixed in Bouin's solution for 24 h. Thereafter, they were prepared for conventional histopathological study, sectioned at 5-µm thickness, and stained with hematoxylin and eosin (H&E) (El-Kossi et al. 2024) and Congo red stain(Rajamohamedsait and Sigurdsson 2012). Ultimately, the stained hippocampus and cerebral cortex sections were photographed using a light microscope coupled with a digital camera at the Faculty of Veterinary Medicine, Assiut University, Egypt, Department of Pathology.

2.13 | Immunohistochemical Analysis

Immunohistochemical detection of p-Tau protein was conducted on formalin-fixed paraffin-embedded brain sections. Sections 4 µm thick from the hippocampus and cerebral cortex were mounted on positively charged slides, deparaffinized, and hydrated in descending grades of ethanol. The activity of endogenous peroxidase was inhibited by blocking it with 3% hydrogen peroxide in methanol. Slides were subjected to anti-rat rabbit polyclonal phosphorylated primary Tau (P-Tau) antibody (Biosource International, Inc., USA, Cat. No. MBS859113, diluted 1:50) after antigen retrieval and blocking nonspecific binding. Detection of primary antibodies was achieved using a biotinstreptavidin detection system with 3,3'-Diaminobenzidine (DAB) as a chromogen. Thereafter, the sections were counterstained with hematoxylin. Negative control was performed by substituting the specific primary antibodies with normal rabbit immunoglobulin (Nashwa Hamad1 2022). P-Tau immune-positive cells showed brown staining of the cytoplasm of the neuronal perikarya.

2.14 | Histomorphometric Analysis

On H&E-stained hippocampal and cerebral cortex sections, quantification of the number of degenerated and necrotic hippocampal neurons in CA1, CA3, and dentate gyrus (DG) subdivisions, as well as the number of degenerated and necrotic cerebral cortical neurons, was accomplished (Ismaeil et al. 2021). In addition, layer thickness of the pyramidal cells in

CA1 and CA3 and granular cells in the DG was assessed. The layer thickness of the pyramidal cells: The distance between 2 imaginary lines drawn from the uppermost to the lowermost pyramidal cells. The layer thickness of the granule cells: The distance between two imaginary lines drawn from the uppermost to the lowermost granule cells (Mandour et al. 2021).

In addition, the number of amyloid plaques in Congo redstained hippocampus and cerebral cortex sections was counted (Snowdon 1997). Moreover, the number of immune-positive neurons in the hippocampus and cerebral cortex was assessed in the immune-stained sections (Shankar et al. 2009).

Morphometric analysis was performed in five high-power fields from three sections of six rats per group using ImageJ software (Wayne Rasband, NIH, Bethesda, Maryland, USA). The count process was performed blindly to ensure accuracy. The results obtained were then statistically analyzed.

2.15 | Statistical Analysis

Afterwards, the Shapiro-Wilk test for normality, as well as one-way and two-way repeated measures of ANOVA, were implemented to assess the quantitative data, followed by Tukey's and Šidák post hoc comparison testing. The results were expressed as the mean \pm standard error. GraphPad Prism, version 8.0.2, was employed to conduct the statistical analysis. A p-value of less than 0.05 was employed to evaluate statistical significance.

3 | Results

3.1 | Effect of RIVA, EMPA, and Their Combination on SCO + HMM-Treated Rats' Memory and Learning

3.1.1 | Y-Maze Spontaneous Alternation Test

In contrast to the control group, the SCO + HMM-induced group successfully reduced the Y-maze's spontaneous alternation and entry count, which led to a low percentage score. Nonetheless, EMPA treatment may result in more spontaneous alternation and total entries, which would raise the percentage score (Figure 1a,b).

3.1.2 | PA Test

Step-through latency was considerably lower in the SCO+HMM group than in the control group (p < 0.0001), suggesting cognitive deficits. Step-through latency increased significantly in the RIVA and EMPA groups compared to the SCO+HMM group (p < 0.0001, p < 0.0001), indicating improvements in memory and learning tasks. Although there were no significant differences between RIVA and EMPA groups, Retention latency times for the RIVA+EMPA group differed significantly compared to each drug alone (p < 0.0001), suggesting that the RIVA+EMPA combination was beneficial (Figure 1c).

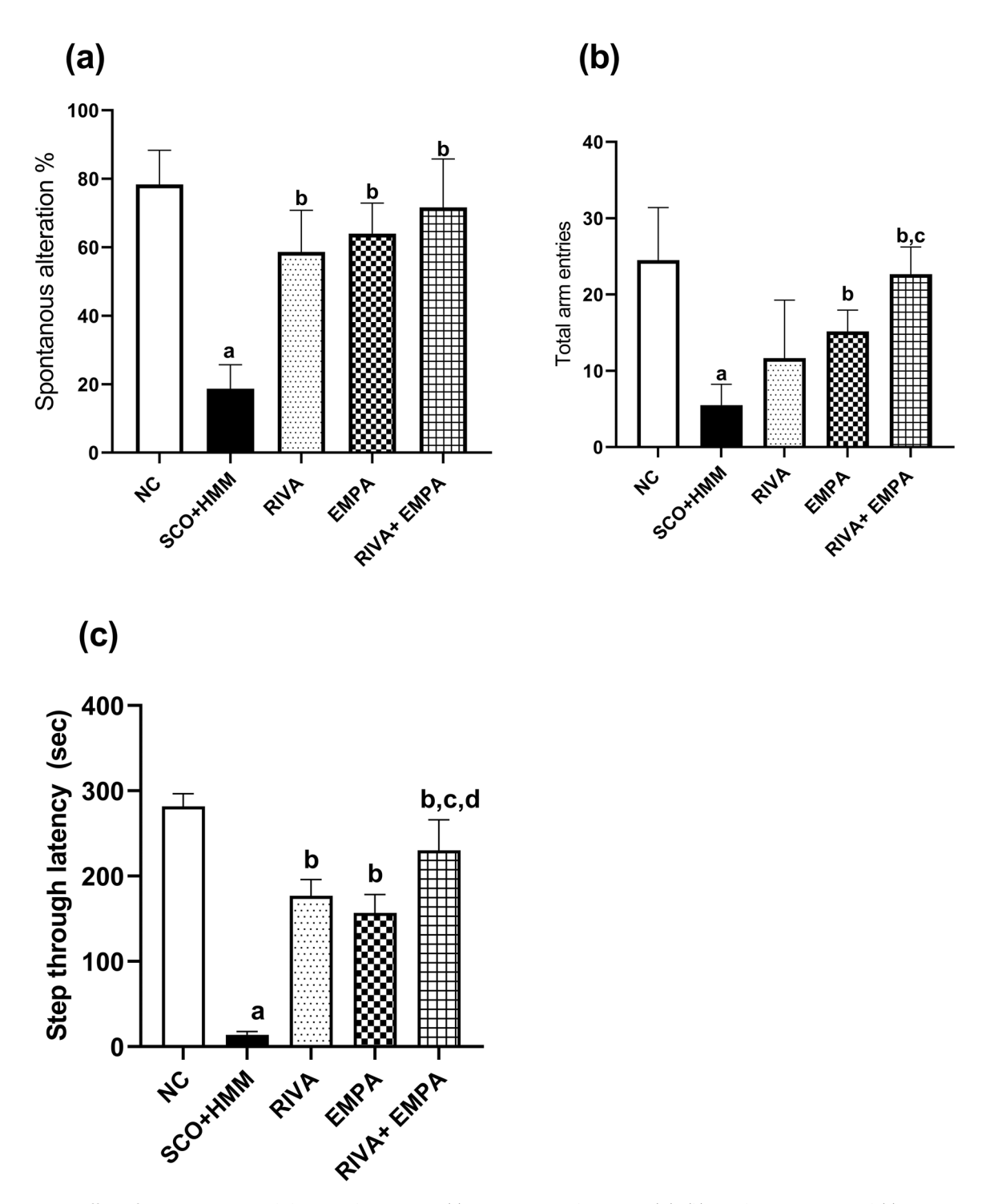


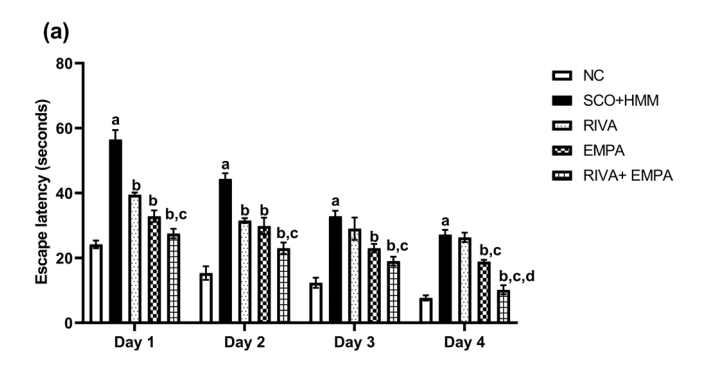
FIGURE 1 | Effect of EMPA, RIVA, and their combination on (a) Spontaneous alternation (%), (b) Total arm entries, and (c) Passive avoidance (PA) test. Step-Through Latency (STL) to enter the dark compartment in seconds during the induction of AD. Data expressed as mean \pm SEM and analyzed using one-way ANOVA followed by Tukey's comparison tests. (a) significant versus NC group, (b) significant versus SCO + HMM, (c) significant versus RIVA, and (d) significant versus EMPA. AD: Alzheimer's disease, NC: Normal control, SCO + HMM: Scopolamine + Heavy metal mixture, RIVA: Rivastigmine, and EMPA: Empagliflozin (n = 6).

3.1.3 | MWM Test

Over the course of the four training days, escape latency constantly decreased, demonstrating improved acquisition behavior across all groups. In MWM, the SCO + HMM group's escape latency to reach the secret platform was noticeably longer than that of the control group. In treated rats, EMPA dramatically

improved escape latency (p < 0.05). Escape latency improved with the RIVA + EMPA combination, though significance was only observed on day 4 (Figure 2a). Comparing the SCO + HMM-induced rats to the control group, the former spent noticeably less time in the target quadrant. (8.833 \pm 1.014 vs. 43.00 ± 1.592 s, respectively; p < 0.0001). Rats treated with EMPA didnot only spent a lot more time in the target quadrant

Drug Development Research, 2025 5 of 17



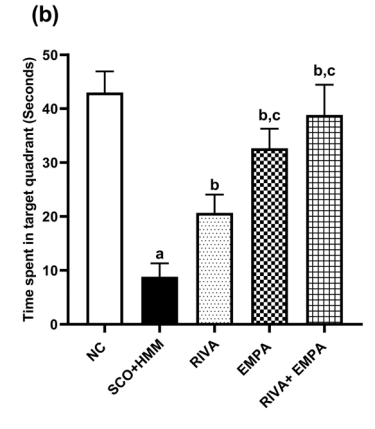


FIGURE 2 | Effect of EMPA, RIVA, and their combination on (a) escape latency (seconds) and (b) Time spent in the target quadrant (seconds) during the induction of AD. Data expressed as mean \pm SEM and analyzed using two-way ANOVA followed by Tukey's comparison tests. (a) significant versus NC group, (b) significant versus SCO + HMM, (c) significant versus RIVA, and (d) significant versus EMPA. AD: Alzheimer's disease, NC: Normal control, SCO + HMM: Scopolamine +Heavy metal mixture, RIVA: Rivastigmine, and EMPA: Empagliflozin (n = 6).

than the SCO + HMM group did $(32.67\pm1.482 \text{ vs.} 8.833\pm1.014 \text{ s},\ p<0.0001)$ but also spent a more significant time than the RIVA group did $(32.67\pm1.482 \text{ vs.} 20.67\pm1.382 \text{ s},\ p<0.0001)$ (Figure 2b).

3.2 | Biochemical Assays

3.2.1 | Effect of RIVA, EMPA, and Their Combination on Pro-Inflammatory and Anti-Inflammatory Mediators in the Hippocampus of Rats

TNF- α and IL-6 levels in the hippocampal areas of diseased rats were noticeably higher than those of healthy control rats. TNF- α tissue levels were 1042 ± 56.22 versus 108.5 ± 3.205 Pg/mg tissue; p < 0.0001; IL-6 tissue levels were 890.8 ± 26.08 versus 90.36 ± 13.42 Pg/mg tissue; p < 0.0001. However, compared to the control, IL-10 levels dropped dramatically (1086 ± 82.89 vs. 121.4 ± 19.19 pg/mg tissue, respectively, p < 0.0001). The EMPAtreated group showed a considerable decline in TNF- α and IL-6 compared to the SCO + HMM group (463.2 ± 30.68 Pg/mg tissue for TNF- α , p < 0.0001; 455.7 ± 26.19 Pg/mg tissue for IL-6, p < 0.0001). On the other hand, IL-10 levels were markedly elevated by EMPA treatment (584.6 ± 48.87 Pg/mg tissue,

p=0.0009). RIVA-treated group failed to outperform the decrease in TNF-α and IL-6 levels achieved by EMPA (663.8 ± 20.22 Pg/mg tissue for TNF-α, p=0.0074, and 658.7 ± 42.29 Pg/mg tissue for IL-6, p=0.0025). In comparison to EMPA alone, the RIVA + EMPA combination significantly reduced TNF-α and IL-6 levels (215.9 ± 18.11 Pg/mg tissue for TNF-α, p=0.0016, and 251.5 ± 19.08 Pg/mg tissue for IL-6, p=0.0024). These results are shown in the supporting (Supporting Information S1: Figure 1a–c).

3.2.2 | Influence of RIVA, EMPA, and Their Combination on the Oxidant/Antioxidant Balance in Diseased Rats' Hippocampal Tissues

The demented rats who received SCO + HMM had considerably higher MDA hippocampus levels and much lower SOD and CAT levels, on opposed to normal control group suggesting that their brains' oxidant/antioxidant balance is seriously disturbed. (9.343 \pm 1.024 vs. 0.7950 \pm 0.0892 nmol/mg tissue, respectively, for MDA, $p < 0.0001;\ 30.76 \pm 3.677$ vs. 212.3 ± 6.632 U/mg tissue, respectively, for SOD, $p < 0.0001,\$ and 0.6930 ± 0.0659 vs. 10.69 ± 0.8289 ng/mg tissue, respectively, for CAT, p < 0.0001). Interestingly, compared to diseased rats, drug-treated groups illustrated a significant change in OS indicator levels in the hippocampus.

Animals treated with EMPA and RIVA + EMPA combination had significantly higher levels of SOD and CAT in their hippocampal tissue compared to SCO + HMM rats (127.6 \pm 5.366 and 153.7 ± 4.182 U/mg tissue for EMPA and RIVA + EMPA combination, respectively, vs. 30.76 ± 3.677 U/mg tissue for SOD, p < 0.0001; 5.273 ± 0.2745 and 7.183 ± 0.2547 ng/mg tissue for EMPA and RIVA + EMPA combination, respectively, vs. 0.6930 ± 0.0659 ng/mg tissue for diseased rats for CAT, p < 0.0001). Furthermore, diseased rats treated with EMPA and RIVA + EMPA combination had considerably lower MDA levels than diseased rats treated with SCO + HMM. (5.220 ± 0.2722) and 2.583 ± 0.5185 nmol/mg tissue for EMPA and RIVA + EMPA combination, p = 0.002 and p < 0.0001 respectively vs. 9.343 ± 1.024 nmol/mg tissue for diseased rats). The drugs' combination showed only a more significant difference in MDA levels as opposed to EMPA alone (p < 0.05). These results are shown in the supporting (Supporting Information S1: Figure 1d-f).

3.2.3 | Impact of RIVA, EMPA, and Their Combination on the Activity of Acetylcholinesterase in Diseased Rats' Hippocampal Tissue

The SCO+HMM group showed a notable rise in AChE content in comparison to the control group. (733.3 \pm 42.86 vs.197.8 \pm 11.35 Pg/mg tissue, respectively, p < 0.0001). In contrast, AChE activity was substantially lower in the EMPA-treated group than in the SCO+HMM group. (389.1 \pm 21.12 Pg/mg tissue, p < 0.0001). The EMPA-treated group also showed a more significant decrease in ACHE activity compared to the RIVA-treated one (531.3 \pm 22.90 Pg/mg tissue for RIVA, p < 0.05) (Figure 3a).

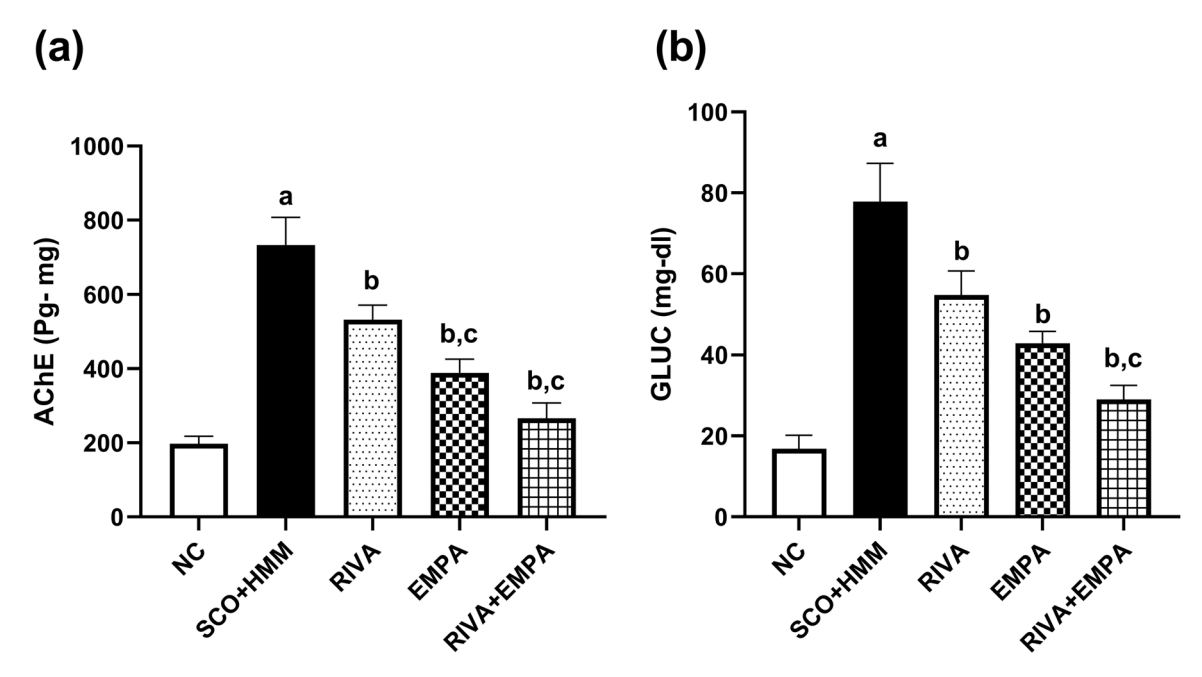


FIGURE 3 | Effect of EMPA, RIVA, and their combination on the level of (a) AChE and (b) GLUC during the induction of AD. Data expressed as mean \pm SEM and analyzed using one-way ANOVA followed by Šidák post hoc comparison tests. (a) significant versus NC group, (b) significant versus SCO + HMM, (c) significant versus RIVA, and (d) significant versus EMPA. AChE: Acetylcholinesterase, GLUC: Glucose, AD: Alzheimer's disease, NC: Normal control, SCO + HMM: Scopolamine + Heavy metal mixture, RIVA: Rivastigmine, and EMPA: Empagliflozin (n = 6).

3.2.4 | Influence of RIVA, EMPA, and Their Combination on GLUC Levels in Diseased Rats' Hippocampal Tissue

Rats induced with SCO + HMM showed dramatically higher brain GLUC levels than the control group (77.84 \pm 1.953 vs. 16.81 \pm 1.953 mg/dL, respectively, p < 0.0001). GLUC levels in the brain declined markedly in RIVA and EMPA-treated groups compared to those in the diseased group (54.80 \pm 3.393 mg/dL, p = 0.0035 for RIVA and 42.81 \pm 1.695 mg/dL, p = 0.0001 for EMPA). The brain GLUC level was significantly lowered by the RIVA and EMPA combination treatment more than by RIVA alone (29.05 \pm 1.973 mg/dL, p = 0.0015) (Figure 3b).

3.2.5 | Impact of RIVA, EMPA, and Their Combination on Glycolytic Enzymes and Glucose Transporters in the Rats' Hippocampus

The SCO + HMM group expressed less LDH-A, PDK-1, and (GLUT)-1, 3 than the control group (p < 0.0001). Both GLUT-1 and GLUT-3 were significantly overexpressed after EMPA therapy in comparison to the SCO + HMM group (p < 0.05). Furthermore, RIVA and EMPA together demonstrated a more substantial elevation in both GLUTs than EMPA by itself (p < 0.05). In comparison to the diseased group, EMPA therapy was able to raise LDH-A and PDK-1 expression, although this increase was not statistically significant for LDH-A. When RIVA is added to EMPA treatment, LDH-A and PDK-1 expression may rise significantly (p < 0.05) in comparison to the diseased group (Figure 4).

3.2.6 | Impact of RIVA, EMBA, and Their Combination on the Histopathological Changes of Diseased Rats

Table 1 demonstrates the number of degenerated and/or necrotic neurons in sections of the hippocampus and cerebral cortex of control and other treated groups. Table 2 shows the layer thickness of pyramidal cells in CA1 and CA3 and granule cells in DG, which could indicate the extent of neuro-degenerative changes.

Hippocampal sections of normal control rats revealed normal histoarchitecture of CA1, CA3, and dentate gyrus (DG) subdivisions with normal neuronal cytomorphology in pyramidal cells, granule cells, polymorphic cells, and molecular layers (Figure 5a-c). On the contrary, the SCO+HMM group exhibited deleterious histopathological changes, which revealed disarranged and loosely packed pyramidal cells in CA1 and CA3, as well as granule cells in DG. Moreover, extensive neuronal degenerative and necrotic changes were evident. The degenerated neurons appeared shrunken with dark cytoplasm, pericellular haloes, and pyknotic nuclei. Whereas the necrotic neurons had cytoplasm with intense eosinophilia and pyknotic nuclei. Some necrotic neurons appeared as ghosts with faded eosinophilia of cytoplasm and vague outlines.

The number of the degenerated and necrotic cells in hippocampal subdivisions of this group revealed significant increase compared to normal control group. However, the layers thickness significantly decreased. Dilated blood capillaries were also noticed (Figure 5d-f). All these alterations were obviously regressed in groups treated with RIVA (Figure 5g-i), EMPA (Figure 5j-i), and RIVA + EMPA (Figure 5m-o) with significant decreased number of degenerated and necrotic cells in CA1,

Drug Development Research, 2025 7 of 17

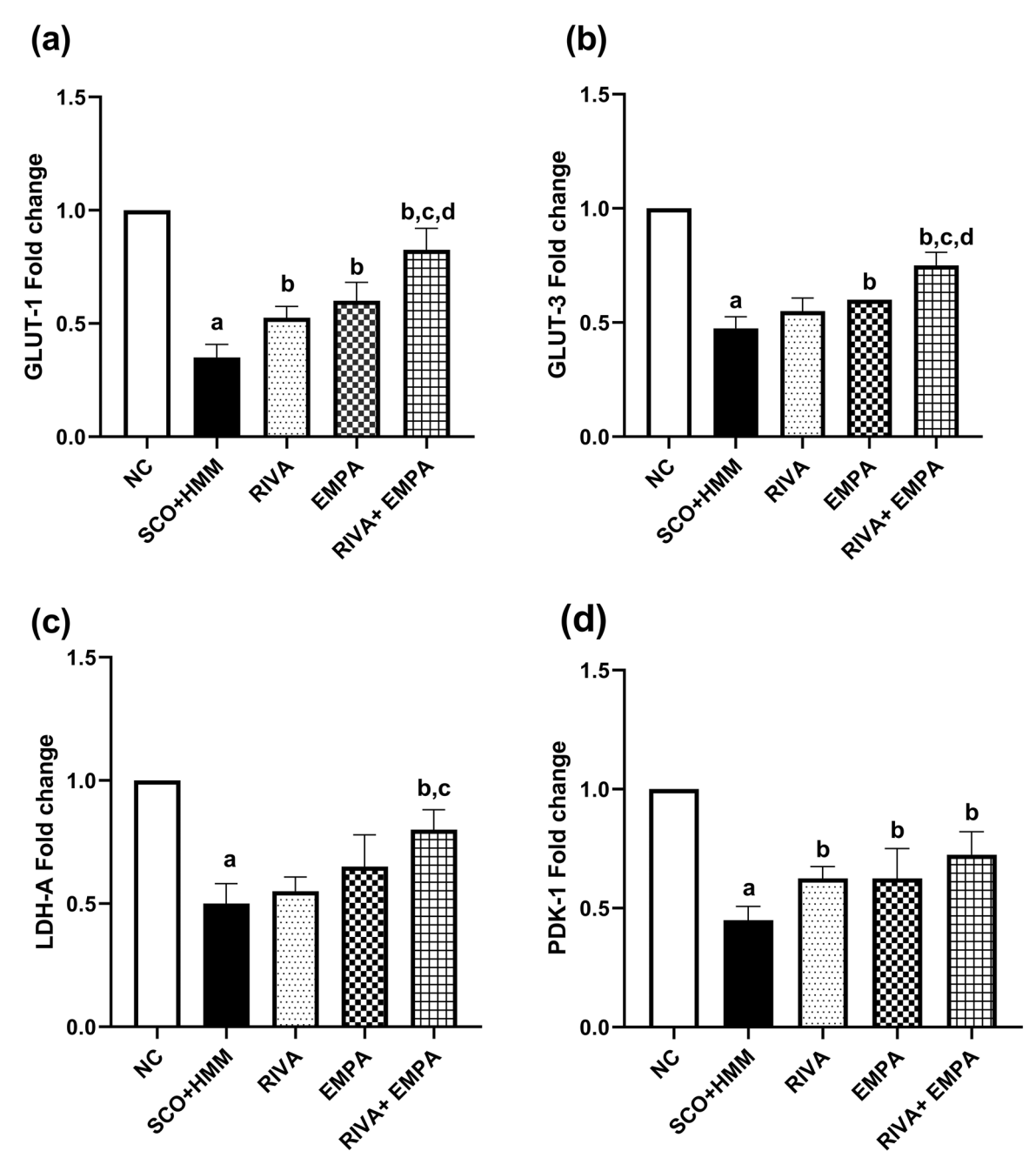


FIGURE 4 | Effect of EMPA, RIVA, and their combination on (a) GLUT-1, (b) GLUT-3, (c) LDH-A, and (d) PDK-1 during the induction of AD. Data expressed as mean ± SEM and analyzed using one-way ANOVA followed by Šidák post hoc comparison tests. a: significant versus NC group, b: significant versus SCO + HMM, c: significant versus RIVA, and d: significant versus EMPA. GLUT-1: glucose transporters-1, GLUT-3: glucose transporters-3, LDH-A: lactate dehydrogenase -A, PDK-1: Pyruvate dehydrogenase kinase-1, AD: Alzheimer's disease, NC: Normal control, SCO + HMM: Scopolamine + Heavy metal mixture, RIVA: Rivastigmine, and EMPA: Empagliflozin (*n* = 4).

CA3, and DG regions compared to SCO + HMM group. On the other hand, the thickness of layers in these treated groups significantly increased. Treatment with RIVA + EMPA significantly reduced the number of degenerated and necrotic neurons in CA1, CA3, and DG and increased the layers thickness relative to the RIVA-treated group. Whereas it decreased the number of degenerated and necrotic neurons significantly in CA1 and CA3 and non-significantly in DG relative to the EMPA-treated group. Furthermore, the layers thickness in RIVA + EMPA group in comparison with EMPA-treated group increased significantly in CA1 and CA3 and non-significantly in DG.

Concerning the cerebral cortex, the normal control rats had normal histomorphology with well-shaped neurons (Supporting Information S1: Figure 2a,f). Meanwhile, sections of the SCO + HMM group showed obvious histopathological alterations expressed by widespread neuronal degeneration with shrunken, deeply stained cytoplasm and pyknotic nuclei. Also, neuronal necrosis with intensely eosinophilic cytoplasm and absent nuclei was evident in most examined sections of this group. There was significant increase in the number of degenerated and necrotic neurons in this group relative to normal control group. Congestion of meningeal and cerebrocortical blood vessels, as well as focal meningeal hemorrhages, were also remarkable findings

TABLE 1 | Mean numbers of degenerated and/or necrotic neurons in H&E-stained hippocampal (CA1, CA3, DG) and cerebral cortical sections.

	Number of degenerated and necrotic neurons			s
	Hippocampus			
Groups	CA1	CA3	DG	Cerebral cortex
NC	0.67 ± 0.33	1.33 ± 0.33	3.83 ± 0.60	0.67 ± 0.42
SCO + HMM	12.67 ± 1.20^{a}	18.67 ± 1.56^{a}	103.70 ± 4.59^{a}	11.00 ± 0.89^{a}
RIVA	5.00 ± 0.58^{b}	7.83 ± 0.60^{b}	62.17 ± 3.99^{b}	5.83 ± 0.54^{b}
EMPA	4.00 ± 0.68^{b}	6.00 ± 0.45^{b}	53.83 ± 3.16^{b}	4.83 ± 0.31^{b}
RIVA + EMPA	1.67 ± 0.21^{bc}	3.67 ± 0.61^{bc}	$11.67 \pm 1.28^{\text{bcd}}$	$\pm 0.48^{\text{bcd}}$

Note: Data are expressed as mean ± SEM and analyzed using one-way ANOVA followed by Šidák post hoc comparison test. a: significant versus NC group, b: significant versus SCO + HMM, c: significant versus RIVA, and d: significant versus EMPA. CA1, CA2, and DG (dentate gyrus) subdivisions of the hippocampus. Normal control (NC), Scopolamine +Heavy metal mixture (SCO + HMM), Rivastigmine (RIVA), Empagliflozin (EMPA).

TABLE 2 | Mean thickness of the pyramidal layer of CA1 and CA3 and thickness of the granular layer of DG in H&E-stained hippocampal sections.

	Layer thickness (μm)			
Groups	CA1	CA3	DG	
NC	63.17 ± 1.19	66.90 ± 1.24	77.10 ± 2.50	
SCO + HMM	35.43 ± 1.42^{a}	30.09 ± 0.89^{a}	38.75 ± 0.91^{a}	
RIVA	40.81 ± 1.23 b	$48.54 \pm 1.25^{\mathrm{b}}$	52.29 ± 1.11^{b}	
EMPA	$41.92 \pm 0.88^{\mathrm{b}}$	50.46 ± 3.42^{b}	65.22 ± 3.48^{bc}	
RIVA + EMPA	$49.58 \pm 0.94^{\text{bcd}}$	$59.44 \pm 2.16^{\text{bcd}}$	$69.87 \pm 0.93^{\rm bc}$	

Note: Data are expressed as mean ± SEM and analyzed using one-way ANOVA followed by Šidák post hoc comparison test. a: significant versus NC group, b: significant versus SCO + HMM, c: significant versus RIVA, and d: significant versus EMPA. CA1, CA2, and DG (dentate gyrus) subdivisions of the hippocampus. Normal control (NC), Scopolamine +Heavy metal mixture (SCO + HMM), Rivastigmine (RIVA), Empagliflozin (EMPA).

(Supporting Information S1: Figure 2b,g). In RIVA-treated rats, there was vascular congestion and a significant reduction in the number of degenerated and necrotic neurons relative to the SCO + HMM group (Supporting Information S1: Figure 2c,h). Similarly, the EMPA-treated group exhibited slight dilatation of cortical blood vessels and significantly diminished neuronal degeneration and necrosis relative to the SCO + HMM group (Supporting Information S1: Figure 2d,i). On the other hand, rats treated with RIVA + EMPA showed marked improvement in the histoarchitecture of the cerebral cortex with slight vascular congestion in some examined sections and significant reduction in the number of degenerated and necrotic neurons compared to SCO + HMM, RIVA, and EMPA groups (Supporting Information S1: Figure 2e,j).

Microscopical examination of Congo red-stained sections showed the absence of amyloid plaque deposition in the hippocampus and cerebral cortex of the normal control group. However, their number significantly increased in the SCO+HMM group compared to the normal control (NC) group. Rats treated with RIVA showed a significant reduction of the deposited amyloid plaques in the hippocampus and cerebral cortex compared to the SCO+HMM group. In the EMPA-treated rats, Congo red stain sections revealed the absence of amyloid plaques in the cerebral cortex and a decrease in their number in the hippocampus compared to the SCO+HMM group. The RIVA+EMPA-treated rats displayed an absence of amyloid

plaque deposition in both hippocampal and cerebral cortical sections (Supporting Information S1: Figure 3).

3.2.7 | Immunohistochemical Expression of P-Tau Protein in the Hippocampus and Cerebral Cortex

The immune positive neurons for p-tau protein had brown colored perikaryal cytoplasm. NC rats showed no p-tau proteinpositive neurons in both the hippocampal pyramidal cell layer and cerebral cortex sections (Figure 6a,f). The SCO + HMM group had many positive p-tau protein neurons in both the pyramidal layer of the hippocampus and the cerebral cortex (Figure 6b,g). The RIVA-treated group revealed some p-tau protein-positive neurons in both the hippocampus and the cerebral cortex (Figure 6c,h). EMPA-treated rats had a few p-tau protein-positive neurons in both the hippocampus and cerebral cortex (Figure 6d,i). RIVA + EMPA-treated rats showed no immunoreaction in the hippocampus and only a few p-tau protein-positive neurons in the cerebral cortex (Figure 6e,j). The number of immune-positive cells in the SCO + HMM group was significantly increased relative to the NC group. The rats treated by RIVA, EMPA, and RIVA + EMPA showed a significant decrease in the number of positive neurons compared to the SCO + HMM group. The EMPA-treated rats displayed a substantial reduction in the number of p-tau protein-positive neurons compared to the RIVA-treated rats. Treatment with

Drug Development Research, 2025 9 of 17

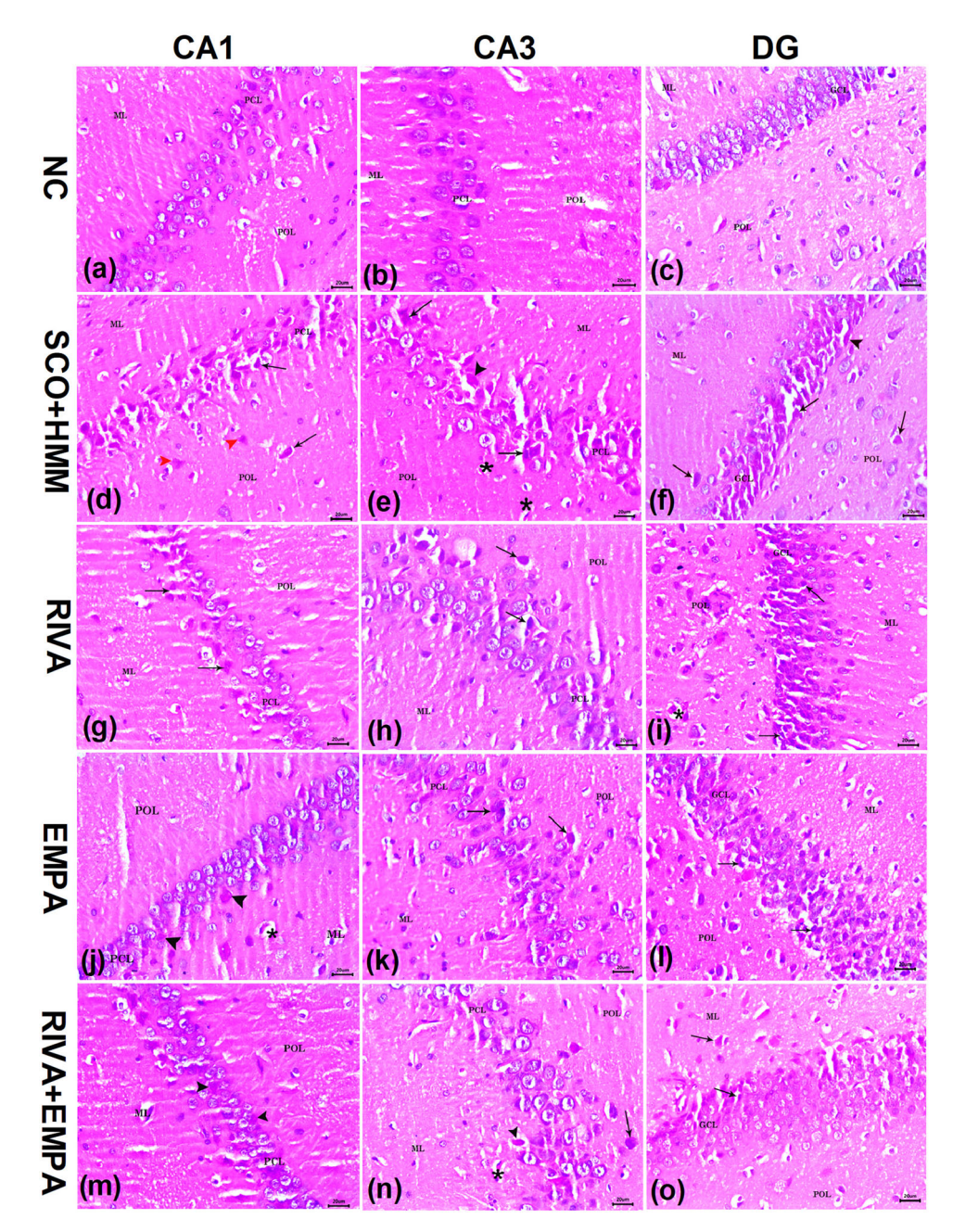


FIGURE 5 | Effect of RIVA, EMPA, and their combination on SCO + HMM-induced histopathological changes in CA1, CA3, and DG subdivisions of the hippocampus. (a-c) NC group, (d-f) SCO + HMM group, (g-i) RIVA group, (j-l) EMPA group, (m-o) RIVA + EMPA group. DG: Dentate gyrus, ML: Molecular layer, PCL: Pyramidal cell layer, POL: Polymorphic layer, GCL: Granule cell layer, degenerated neurons (arrow), necrotic neurons (black arrowhead), ghost necrotic neurons (red arrowhead), dilated blood capillaries (asterisk). NC: Normal control, SCO + HMM: Scopolamine + Heavy metal mixture, RIVA: Rivastigmine, and EMPA: Empagliflozin. H&E stain. Bar = 20 μm.

RIVA + EMPA significantly reduced their number in comparison with RIVA and EMPA-treated groups (Figure 6k,l).

4 | Discussion

A progressive age-related neurodegenerative decline in cognitive abilities, AD has a significant influence on memory and learning (Anoush et al. 2025). Sixty percent to 80% of all cases of dementia are caused by this neurodegenerative illness, making it the most prevalent (Kamatham et al. 2024).

The exact cause of AD has not yet been determined up till now. Cholinergic dysfunction (Hampel et al. 2018), $A\beta$ aggregation (Ratan et al. 2023), tau hyperphosphorylation (Murakami and Lacayo 2022), OS (Roy et al. 2023), and neuroinflammation (Rizzo et al. 2022) are among the hypotheses that have been developed to explain the pathogenesis mechanisms of AD. Moreover, metabolic (Argentati et al. 2020) and synaptic (Ratan et al. 2023) also contribute to this pathogenesis. In AD, increased AChE activity causes OS spikes and the production of ROS, which in turn causes brain lipid peroxidation and, ultimately, faster $A\beta$ aggregation (Tang 2019). This process leads to

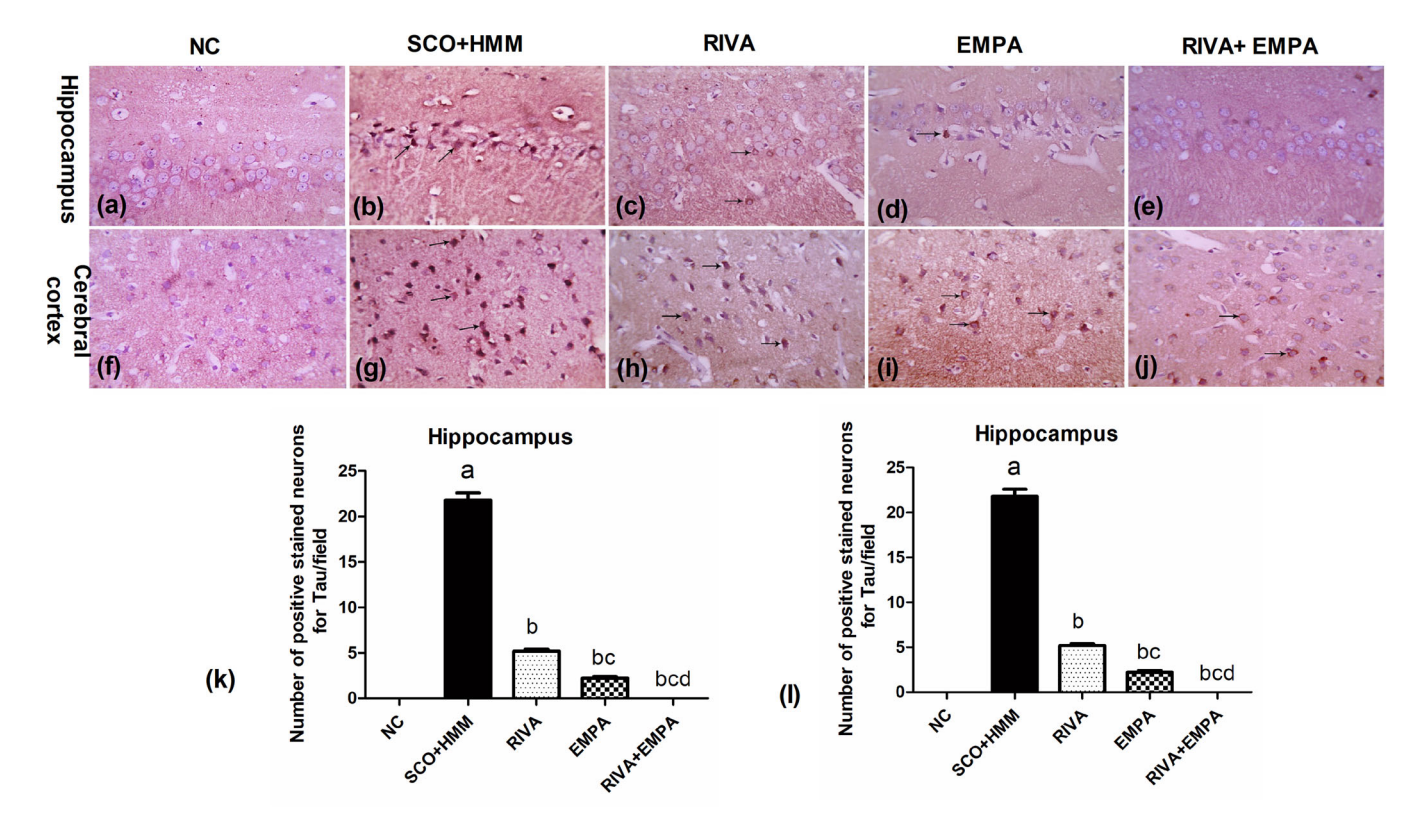


FIGURE 6 | Effect of RIVA, EMPA, and their combination on the immune expression of p-tau protein in the hippocampus (upper panel) and cerebral cortex (lower panel). The immune positive neurons had brown colored perikaryal cytoplasm (arrow). (a, f) NC group, (b, g) SCO + HMM group, (c, h) RIVA treated group, (d, i) EMPA treated group, (e, j) RIVA + EMPA treated group. Bar = $20 \,\mu\text{m}$. (k, l) depicting mean \pm SEM of p-tau protein positive neuron numbers in both the hippocampus and the cerebral cortex. Data was analyzed using one-way ANOVA followed by Šidák post hoc comparison test. a: significant versus NC group, b: significant versus SCO + HMM, c: significant versus RIVA, and d: significant versus EMPA. NC: Normal control, SCO + HMM: Scopolamine + Heavy metal mixture, RIVA: Rivastigmine, and EMPA: Empagliflozin.

neurodegeneration and neuroinflammation, primarily in glial cells, and ultimately to memory loss and cognitive dysfunction (Mishra and Thakur 2022).

Four AChE inhibitors: tacrine, donepezil, RIVA, and galantamine, and one N-methyl-D-aspartate (NMDA) receptor antagonist: memantine, are currently the most accepted pharmacological options for AD. Both AChE and butyrylcholinesterase (BuChE) control ACh breakdown in the brain. With AD progression, BuChE activity rises in brain areas such as the hippocampus and temporal cortex, but AChE activity decreases, highlighting the critical role of BuChE in maintaining cholinergic balance (Mesulam et al. 2002). Although initial treatments targeted only AChE, subsequent evidence emphasizes the therapeutic importance of dual inhibition of both types of ChE for AD management (Lanteri et al. 2006). RIVA achieves this through its distinctive reversible inhibition of both enzymes (Hirosawa et al. 2020), thereby sustaining cholinergic transmission and enhancing Ach availability as the disease progresses, in addition to its longer duration of action (Marucci et al. 2021).

Moreover, the transdermal patch formulation of RIVA offers continuous drug delivery with fewer gastrointestinal adverse effects, improving treatment adherence and tolerability (Cuadros Cuadros 2024). RIVA's unique mechanism of action supports cognitive function and daily living activities more

effectively than memantine, which primarily mitigates glutamate-related excitotoxicity in later stages of AD, as evidenced clinically by Wang et al. (2015) in addition to possible disease-modifying actions through α -secretase upregulation, interrupting the production of toxic A β in AD (Jamshidnejad-Tosaramandani et al. 2021). Real-world studies further demonstrate improved outcomes and even lower mortality rates among dementia patients treated with RIVA (Havreng-Théry et al. 2024). Taken together, these findings suggest that rivastigmine is better suited for patients with mild to moderate AD, while memantine provides greater benefit in more advanced stages or when combined with AChE inhibitors (Knorz and Quante 2022).

Since the conventional anti-AD agents act primarily as symptomatic treatments rather than disease-modifying therapies and cannot halt the inevitable progression of AD (Nazam et al. 2021) alongside with increasing prevalence of AD, there is a growing need to expand the testing of new mechanistic hypotheses to approach the disease from various perspectives (Stanciu et al. 2023) and repurpose commonly used medications that can effectively manage the disease while minimizing side effects. Beyond their glucose metabolism-correcting effect, SGLT-2is have the ability to improve brain metabolism and regeneration.

The mechanisms by which the physical and chemical properties of SGLT-2is regulate their transportation in the CNS are still not

fully elucidated, but their low molecular weight and high lipidsolubility enable SGLT-2is to cross the BBB (Ali et al. 2025). Intrensigly, neuroinflammation, oxidative stress, and apoptosis of BBB microvascular endothelial cells, which are associated with neurological disorders, including Parkinson's disease and AD (Pan and Nicolazzo 2018) lead to BBB impairment, which contributes to further penetration of SGLT-2is (Dong et al. 2022). These facts guarantee the use of SGLT-2is to improve memory and cognition in those with moderate cognitive impairment or dementia and reduce the incidence of dementia by 42% (Youn et al. 2024). According to Pawlos et al.(2021) and Xu et al. (2022) this impact is ascribed to their capacity to inhibit AChE as well. Furthermore, SGLTi therapy markedly reduced AD pathology, such as tau phosphorylation and senile plague density, in earlier research using murine models (Hierro-Bujalance et al. 2020). Additionally, SGLTis have pleiotropic actions that could improve cognitive impairment, including anti-inflammatory, anti-atherosclerotic, antioxidant, and neuroprotective properties (Sim et al. 2021). Moreover, compared to metformin, EMPA showed a neuroprotective effect in a rat model of acute cerebral ischemia (Simanenkova et al. 2024). Accordingly, the potential neuroprotective effects of EMPA monotherapy and the RIVA+ EMPA combination in SCO + HMM-induced AD were investigated in our study.

Numerous experimental models resembling AD exist, each with a distinct physiological and pathological foundation. One of the most often utilized models in neurodegenerative research to assess the effectiveness of anti-amnesic medications is the SCOinduced AD-like model in rodents. A modified SCO + HMM model was employed in our study, as described by Ashok and Rai (2023) and Assi et al. (2023), who discovered that rats given a daily mixture of As, Cd, and Pb in drinking water developed notable AD-like alterations. Regrettably, the traditional SCO model has several limitations in its ability to mimic AD in humans. SCO has the characteristic ability to induce tau hyperphosphorylation and amyloid plaque formation, both of which are closely linked to AD pathogenesis. This causes memory loss in rodents that resembles the deficits observed in AD (Mostafa et al. 2016). Scopolamine is a muscarinic receptor antagonist that obstructs cholinergic neurotransmission, leading to memory deficits in rodents (Tang 2019a). On the other hand, the daily consumption of a combination of arsenic (As), cadmium (Cd), and lead (Pb) resulted in Notable changes that were pathognomonic of AD. Heavy metals uptake in the nervous system is detrimental due to their potential to induce OS, disrupt mitochondrial function, and impede the activity of numerous enzymes (Ashok et al. 2015; Islam et al. 2022).

Systemic SCO administration has been shown in numerous experimental studies to cause AD by elevating AChE levels (Demirci et al. 2017; Anoush et al. 2022), OS (Rahman et al. 2019; Yadang et al. 2020), neuroinflammation, neuronal apoptosis, and mitochondrial dysfunction (Foudah et al. 2023), all of which impair learning acquisition and consolidation processes (Amoah et al. 2023). In agreement with these findings, our results demonstrate that SCO + HMM receiving rats exhibited a significant memory decline as evidenced by increased escape latency of the probe trial and decreased time spent in the target quadrant of MWM test, as well as a shorter

STL of PA test along with a reduced number of entries and spontaneous alternation of the Y-maze test leading to a low percentage score. It's interesting to note that our treatment plans, which included EMPA alone and RIVA + EMPA in combination, significantly decreased the probe trial's escape latency while significantly increasing the amount of time spent in the target quadrant in the MWM test. The STL in the PA task was prolonged by the same treatment regimens, indicating that they supported the cognitive processes involved in memory retrieval.

The Y-maze test also displayed more entries and spontaneous alternation in these treated groups, which resulted in a high percentage score. Remarkably, compared to EMPA alone, the RIVA + EMPA combination resulted in a more substantial rise in STL in the PA test, indicating greater progress in memory and learning tasks. According to the results of these behavioral tests, EMPA not only protects rats from SCO-HMM-induced deficits in spatial learning and memory when administered alone, but it also strengthens the neuroprotective effect of RIVA when administered concurrently. Consistent with our findings, Abdel-lah et al. (2025) indicated that rats treated with EMPAmemantine combination had a significantly lower escape latency and spent more time in the target quadrant in MWM than SCO-induced rats given memantine or EMPA alone. Also, Anoush et al. (2025) found that rats treated with EMPAdonepezil (DON) in combination had a significantly lower escape latency and spent more time in the target quadrant in MWM than SCO-induced rats given DON or EMPA alone.

Additionally, another study carried out by Chen et al.(2023) demonstrated that EMPA therapy corrected impaired memory performance in mice fed a high-fat diet by improving synaptic plasticity and neural projection development. Similarly, numerous studies have found that dapagliflozin (DAPA) increases the time spent in the target quadrant of the MWM test (Sa-nguanmoo et al. 2017; Abd Elmaaboud et al. 2023) and decreases the time required to reach the target quadrant (Nur Hazaryavuz et al. 2022; Samman et al. 2023). This suggests that DAPA eliminated the delirious effects on acquisition learning in addition to increasing impulsive changes and the number of arm accesses of the Y-maze test, indicating improved working memory and persistent cognition (Samman et al. 2023). DAPA did not, however, improve the latency time in the PA test, demonstrating its inability to improve knowledge recall (Nur Hazaryavuz et al. 2022). Likewise, a research study by Arafa et al. (2017) found that canagliflozin enhanced cognitive abilities in the Y-maze and MWM tests, just like galantamine did. The current study's findings indicate that EMPA treatment ameliorated cognitive function impairment in the diseased rats induced by SCO + HMM.

Since the results of a number of clinical and experimental studies suggested that cholinergic imbalance, OS, neuroin-flammation, and AD are related, we investigated this hypothesis in our study. We found that cholinergic dysfunction, OS, and neuroinflammation were associated with the induction of AD in rats receiving SCO+HMM, as evidenced by elevated AChE activity, MDA and pro-inflammatory cytokines (TNF- α and IL-6) levels in addition to the decreased levels of the antioxidant enzymes (SOD and CAT) and the anti-inflammatory cytokine

(IL-10) in the hippocampal homogenates of these rats compared to their normal surrogates. Our results are in alignment with numerous previous studies, which reported that SCO administration to rats and mice leads to the augmentation of AchE activity and an imbalance of the brain oxidative status (Karthivashan et al. 2018, 2019; Bashir et al. 2023) as reflected by increased AChE activity, MDA, TNF-α, IL-1β, and IL-6 levels, as well as decreased antioxidant enzyme levels (GSH, SOD, CAT, and GPx). On the other hand, our therapeutic regimens, including EMPA as a monotherapy and in combination with RIVA, mitigated these deleterious indicators, with a more pronounced effect on MDA, TNF-α, and IL-6 levels with the combination regimen. Furthermore, our study results indicate that canagliflozin, similar to galantamine, decreases AChE activity and improves cognitive dysfunction in SCO-treated rats (Arafa et al. 2017). Also, DAPA reduced AChE activity in rats receiving AlCl₃ (Samman et al. 2023).

Additionally, EMPA, directly or indirectly, via its antioxidant activity, may restore brain GSH and normalize MDA and CAT levels in SCO-treated rats, according to Anoush et al. (2025). Supporting our study results, a study carried out by Heimke et al. (2022) showed that in an experimental model of neuroinflammation in rats induced by lipopolysaccharide, EMPA decreased the production of pro-inflammatory mediators, corroborating the potential anti-inflammatory actions of EMPA on microglia. Additionally, in a combined mouse model for AD and T2DM, EMPA has been suggested to enhance cognitive impairment and lower vascular inflammation (Hierro-Bujalance et al. 2020). Along with other inflammatory markers, such as IL-1β, IL-6, IL-18, and transforming growth factor beta 1 (TGF-β1), DAPA demonstrated a beneficial anti-inflammatory effect by reducing NF-kB activity in the brain, restoring the antioxidant enzyme defense system, and ameliorating the inflammatory process in SCO + HMM-treated rats. Accordingly, in the current study, hippocampus cholinergic neurotransmission, oxidative stress, and neuroinflammation could be introduced as proposed neuroprotective mechanisms of EMPA in the SCO-induced AD model.

The main constituents of NFTs are hyperphosphorylated aggregated tau formations, which are a pathogenic hallmark observed in the brains of animals and AD patients (Liu et al. 2004; Liu et al. 2008; Liu et al. 2020). Because microglia are more sensitive to NFTs than amyloid plaques, their development and accumulation cause neurodegeneration (Costa et al. 2023) and inflammatory reactions in the brain (Ohm et al. 2021). Therefore, one promising approach for possible disease-modifying therapies is to target aberrant tau aggregation and the downstream effects that are linked to it (Congdon and Sigurdsson 2018). Our findings also indicated that the p-tau level in the total brain area analyzed for SCO + HMM rodents that received the RIVA + EMPA combination decreased significantly. It is important to note that no prior research has examined the impact of this combination on the pathological hallmarks of AD. Nevertheless, previous reports have demonstrated the efficacy of EMPA alone in addressing these hallmarks (Hierro-Bujalance et al. 2020; Hierro-Bujalance and Garcia-Alloza 2024). It has been demonstrated that DAPA, another member of the SGLT1 family, has the ability to decrease the accumulation of Aβ and tau hyperphosphorylation in the brains of diabetic mice. This presumably occurs as a

result of its influence on glucose metabolism, insulin signaling, and neuroinflammation effects (Sim et al. 2023).

Glucose is the primary source of energy that neurons and astrocytes in the brain use to obtain their energy. Intracellular oxidative catabolism and glucose transport into brain cells via the blood-brain barrier (BBB) are the two components of cerebral glucose metabolism. Neurons are entirely dependent on glucose uptake via glucose transporters because they are unable to produce glucose themselves. Altering this cerebral metabolism encourages the development of metabolic disturbances that are emphasized in the brains of AD patients. It appears that insulin resistance and deficiencies in glucose transporters may be associated with glucose transport abnormalities. Reduced GLUT-1 and GLUT-3 levels in certain disorders, like AD, may limit glucose-transporting ability, which results in decreased glucose uptake. This impairment seems to be a contributing factor to neurodegeneration. Furthermore, because the glycolytic enzymes LDH and PDK are significantly reduced in AD, neurons are unable to increase their energy production through the glycolytic pathway. Upregulated oxidative phosphorylation, mitochondrial dysfunction, increased Aβ sensitivity, synaptic degradation, nerve cell death, and eventually cognitive impairment can all result from this deficit. A significant abnormality in the early stages of AD is glucose hypometabolism, which is brought on by a reduction in glucose uptake (Kodam et al. 2023).

Enhancing brain glucose transport may be a likely therapeutic objective for treating AD since GLUT-1 and GLUT-3 levels were markedly reduced in AD. Resistance to A β and decreased mitochondrial activity can result from elevated levels of PDK-1 and LDH-A (Babylon et al. 2022). Since these glycolytic enzymes are thought to be essential for protecting cells from A β toxicity, overexpression of either PDK or LDH enzymes in nerve cell lines suppresses mitochondrial respiration and confers tolerance to A β and other neurotoxins (Babylon et al. 2022).

As previously mentioned, GLUT is downregulated in AD (Erdogan et al. 2018). As a result, targeting GLUT may be advantageous. Both intracellular GLUC levels and absorption were improved by SGLTi-dependent GLUT-1,3 overexpression (Mustroph et al. 2019) PDK and LDH have also been demonstrated to be downregulated in a transgenic AD mouse model. Additionally, it was found that when ALCL3 induced AD in rats, there was a downregulation of GLUT-1, LDH-A, and PDK-1 expression compared to the control group. Further, treatment with DAPA significantly increased the expression of PDK-1 and LDH-A genes compared to the AlCl₃ group. Our investigation revealed that GLUT-1,3 levels were upregulated in the SCO + HMM-induced animals receiving EMPA, consistent with previous findings. This effect was more pronounced when the RIVA + EMPA combination was administered. Moreover, our study revealed that EMPA treatment decreased the elevated brain glucose levels in the SCO-HMM group, and this agrees with a study carried out by Samman et al. (2023) who concluded that DAPA decreased the elevated brain glucose levels in AlCl3treated rats. This may improve the glucose-transporting ability, which would promote glucose metabolism and absorption, and eventually alleviate cognitive dysfunction.

Consistently, in the current study, the EMPA and RIVA + EMPA combination-treated groups showed upregulated levels

of LDH-A and PDK-1 compared to the SCO-HMM-treated group, with a more significant effect observed when using the combination regimen. These results coincide with previous research demonstrating that the administration of SGLTis elevated LDH-A, which may be the outcome of the counteraction of elevated levels of inflammatory cytokines and the amelioration of insulin resistance (Safhi et al. 2018).

5 | Conclusion

In conclusion, we conducted the current study to evaluate the neuroprotective potential of EMPA monotherapy and the RIVA + EMPA combination against the SCO + HMM AD-like model in rats, and to investigate the underlying mechanistic approaches mediating this effect. Based on the results presented here, EMPA significantly reduced the pathological features associated with SCO + HMM-induced AD, providing evidence of its neuroprotective properties through supposedly enhancing cognition, learning, and memory capacities, as suggested by the results of the three behavioral tests, which were used in this study, along with biochemical, real-time PCR, and histopathological changes. Accordingly we can assume that neuroprotective potential of EMPA could be attribute to the following pathways: (1) lowering AChE levels, (2) diminishing tau phosphorylation, (3) modulating markers of OS, (4) modulating pro-inflammatory cytokines and anti-inflammatory mediators (5) decreasing brain blood glucose levels and (6) enhancing cerebral glucose metabolism by upregulation of glycolytic enzymes, as well as GLUTs.

Author Contributions

E.S.A, N.H, M.G.G, and A.F.T conceived and designed the research, data collection, original draft, and methodology, conducted the experiments, analyzed the study, and wrote the manuscript. H.S.S, W.H.M, A.H.A and M.A.F contributed to data collection, biochemical analysis, manuscript writing, and results interpretation. A.A and F.Y.A.A contributed to data collection, original draft, and methodology. N.H contributed to histopathological and immunohistochemical evaluations. All authors read and approved the final manuscript.

Acknowledgments

The authors have nothing to report.

Ethics Statement

This study was approved by the Assiut University, Faculty of Pharmacy's ethical committee with approval number (05-2024-028).

Conflicts of Interest

The authors declare no conflicts of interest.

Data Availability Statement

Data will be made available on request.

References

Abd Elmaaboud, M. A., R. S. Estfanous, A. Atef, et al. 2023. "Dapagli-flozin/Hesperidin Combination Mitigates Lipopolysaccharide-Induced Alzheimer's Disease in Rats." *Pharmaceuticals* 16, no. 10: 1370. https://doi.org/10.3390/ph16101370.

Abdel-Aal, R. A., A.-A. A. Assi, and B. B. Kostandy. 2011. "Memantine Prevents Aluminum-Induced Cognitive Deficit in Rats." *Behavioural Brain Research* 225, no. 1: 31–38. https://doi.org/10.1016/j.bbr.2011. 06.031.

Abdel-lah, E. S., H. S. Sherkawy, W. H. Mohamed, et al. 2025. "Empagliflozin and Memantine Combination Ameliorates Cognitive Impairment in Scopolamine + Heavy Metal Mixture-Induced Alzheimer's Disease in Rats: Role of AMPK/mTOR, BDNF, BACE-1, Neuroinflammation, and Oxidative Stress." *Inflammopharmacology* 33: 3479–3498. https://doi.org/10.1007/s10787-025-01755-5.

Ahmed, S., M. M. El-Sayed, M. A. Kandeil, and M. M. Khalaf. 2022. "Empagliflozin Attenuates Neurodegeneration Through Antioxidant, Anti-Inflammatory, and Modulation of α -synuclein and Parkin Levels in Rotenone-Induced Parkinson's Disease in Rats." *Saudi Pharmaceutical Journal* 30, no. 6: 863–873. https://doi.org/10.1016/j. jsps.2022.03.005.

Alam, S., M. K. Hasan, S. Neaz, N. Hussain, M. F. Hossain, and T. Rahman. 2021. "Diabetes Mellitus: Insights From Epidemiology, Biochemistry, Risk Factors, Diagnosis, Complications and Comprehensive Management." *Diabetology* 2, no. 2: 36–50. https://doi.org/10.3390/diabetology2020004.

Alhakamy, N. A., E. A. Aljehani, A. B. Abdel-Naim, et al. 2024. "Development, Optimization, and Evaluation of Empagliflozin Nanoemulsion for the Management of Neuroinflammation Associated Alzheimer's Disease." *Journal of Drug Delivery Science and Technology* 93: 105425. https://doi.org/10.1016/j.jddst.2024.105425.

Ali, M. A., H. E. Michel, E. T. Menze, M. G. Tadros, and S. A. Wahdan. 2025. "The Potential Neuroprotective Effect of Empagliflozin Against Depressive-Like Behavior Induced by Chronic Unpredictable Mild Stress in Rats: Involvement of NLRP3 Inflammasome." *European Journal of Pharmacology* 998: 177525. https://doi.org/10.1016/j.ejphar. 2025.177525.

Amoah, V., P. Atawuchugi, Y. Jibira, et al. 2023. "Lantana camara Leaf Extract Ameliorates Memory Deficit and the Neuroinflammation Associated With Scopolamine-Induced Alzheimer's-Like Cognitive Impairment in Zebrafish and Mice." *Pharmaceutical Biology* 61, no. 1: 825–838. https://doi.org/10.1080/13880209.2023.2209130.

Anoush, M., N. Taghaddosi, Z. Bokaei Hosseini, et al. 2025. "Neuroprotective Effects of Empagliflozin Against Scopolamine-Induced Memory Impairment and Oxidative Stress in Rats." *IBRO Neuroscience Reports* 18: 163–170. https://doi.org/10.1016/j.ibneur. 2025.01.008.

Anoush, M., N. Tayebi, S. Bijani, M. Ebrahimi, A. Yazdinezhad, and M. J. Hosseini. 2022. "Thymus Daenensis Extract Prevents Scopolamine-Induced Memory Impairment Through Declining Oxidative Stress in Rats." *Acta Neurobiologiae Experimentalis* 82, no. 3: 380–388. https://doi.org/10.55782/ane-2022-036.

Arafa, N. M. S., E. H. A. Ali, and M. K. Hassan. 2017. "Canagliflozin Prevents Scopolamine-Induced Memory Impairment in Rats: Comparison With Galantamine Hydrobromide Action." *Chemico-Biological Interactions* 277: 195–203. https://doi.org/10.1016/j.cbi.2017.08.013.

Argentati, C., I. Tortorella, M. Bazzucchi, C. Emiliani, F. Morena, and S. Martino. 2020. "The Other Side of Alzheimer's Disease: Influence of Metabolic Disorder Features for Novel Diagnostic Biomarkers." *Journal of Personalized Medicine* 10, no. 3: 115. https://doi.org/10.3390/jpm10030115.

Ashok, A., and N. K. Rai. 2023. "Metal Mixture-Induced Non-Transgenic Animal Model of Alzheimer's Disease: Pros and Cons." *Pre-Clinical Research* 1, no. 1: 7768. https://doi.org/10.4081/pcr.2023.7768.

Ashok, A., N. K. Rai, S. Tripathi, and S. Bandyopadhyay. 2015. "Exposure to As-, Cd-, and Pb-Mixture Induces $A\beta$, Amyloidogenic APP Processing and Cognitive Impairments via Oxidative Stress-Dependent Neuroinflammation in Young Rats." *Toxicological Sciences* 143, no. 1: 64–80. https://doi.org/10.1093/toxsci/kfu208.

Assi, A.-A., S. Abdelnabi, A. Attaai, and R. B. Abd-ellatief. 2022. "Effect of Ivabradine on Cognitive Functions of Rats With Scopolamine-Induced Dementia." *Scientific Reports* 12, no. 1: 16970. https://doi.org/10.1038/s41598-022-20963-5.

Assi, A.-A., M. M. Y. Farrag, D. M. Badary, E. A. H. Allam, and M. A. Nicola. 2023. "Protective Effects of Curcumin and *Ginkgo biloba* Extract Combination on a New Model of Alzheimer's Disease." *Inflammopharmacology* 31, no. 3: 1449–1464. https://doi.org/10.1007/s10787-023-01164-6.

Babylon, L., F. Schmitt, Y. Franke, T. Hubert, and G. P. Eckert. 2022. "Effects of Combining Biofactors on Bioenergetic Parameters, Aβ Levels and Survival in Alzheimer Model Organisms." *International Journal of Molecular Sciences* 23, no. 15: 8670. https://doi.org/10.3390/iims23158670.

Bashir, D. J., S. Manzoor, M. Sarfaraj, et al. 2023. "Magnoflorine-Loaded Chitosan Collagen Nanocapsules Ameliorate Cognitive Deficit in Scopolamine-Induced Alzheimer's Disease-Like Conditions in a Rat Model by Downregulating IL-1β, IL-6, TNF-α, and Oxidative Stress and Upregulating Brain-Derived Neurotrophic Factor and DCX Expressions." *ACS Omega* 8, no. 2: 2227–2236. https://doi.org/10.1021/acsomega.2c06467.

Borikar, S. P., G. V. Chitode, D. N. Tapre, D. K. Lokwani, and S. P. Jain. 2024. "Empagliflozin Ameliorates Olfactory Bulbectomy-Induced Depression by Mitigating Oxidative Stress and Possible Involvement of Brain Derived Neurotrophic Factor in Diabetic Rats." *International Journal of Neuroscience* 135, no. 9: 1010–1022. https://doi.org/10.1080/00207454.2024.2342973.

Chen, X., S. Chen, Z. Li, et al. 2023. "Effect of Semaglutide and Empagliflozin on Cognitive Function and Hippocampal Phosphoproteomic in Obese Mice." *Frontiers in Pharmacology* 14: 975830. https://doi.org/10.3389/fphar.2023.975830.

Congdon, E. E., and E. M. Sigurdsson. 2018. "Tau-Targeting Therapies for Alzheimer Disease." *Nature Reviews Neurology* 14, no. 7: 399–415. https://doi.org/10.1038/s41582-018-0013-z.

Costa, I., D. J. Barbosa, V. Silva, et al. 2023. "Research Models to Study Ferroptosis's Impact in Neurodegenerative Diseases." *Pharmaceutics* 15, no. 5: 1369. https://doi.org/10.3390/pharmaceutics15051369.

Cuadros Cuadros, R. F. 2024. "Parches transdérmicos de rivastigmina para la enfermedad de Alzheimer en Colombia: estudio de experiencia y percepción." *Acta Neurológica Colombiana* 40, no. 4: 1786. https://doi.org/10.22379/anc.v40i4.1786.

Cunnane, S., S. Nugent, M. Roy, et al. 2011. "Brain Fuel Metabolism, Aging, and Alzheimer's Disease." *Nutrition* 27, no. 1: 3–20. https://doi.org/10.1016/j.nut.2010.07.021.

Demirci, K., M. Nazıroğlu, İ. İ. S. Övey, and H. Balaban. 2017. "Selenium Attenuates Apoptosis, Inflammation and Oxidative Stress in the Blood and Brain of Aged Rats With Scopolamine-Induced Dementia." *Metabolic Brain Disease* 32, no. 2: 321–329. https://doi.org/10.1007/s11011-016-9903-1.

Domínguez, R. O., E. R. Marschoff, S. E. González, M. G. Repetto, and J. A. Serra. 2012. "Type 2 Diabetes and/or Its Treatment Leads to Less Cognitive Impairment in Alzheimer's Disease Patients." *Diabetes Research and Clinical Practice* 98, no. 1: 68–74. https://doi.org/10.1016/j.diabres.2012.05.013.

Dong, M., S. Wen, and L. Zhou. 2022. "The Relationship Between the Blood-Brain-Barrier and the Central Effects of Glucagon-Like Peptide-1 Receptor Agonists and Sodium-Glucose Cotransporter-2 Inhibitors." *Diabetes, Metabolic Syndrome and Obesity: Targets and Therapy* 15: 2583–2597. https://doi.org/10.2147/DMSO.S375559.

El-Kossi, D. M. M. H., S. S. Ibrahim, K. M. A. Hassanin, N. Hamad, N. A. Rashed, and A. Abdel-Wahab. 2024. "Ameliorative Effects of Zinc Oxide, in Either Conventional or Nanoformulation, Against Bisphenol A Toxicity on Reproductive Performance, Oxidative Status, Gene

Expression and Histopathology in Adult Male Rats." *Biological Trace Element Research* 202, no. 5: 2143–2157. https://doi.org/10.1007/s12011-023-03830-w.

Erdogan, M. A., D. Yusuf, J. Christy, et al. 2018. "Highly Selective SGLT2 Inhibitor Dapagliflozin Reduces Seizure Activity in Pentylenetetrazol-Induced Murine Model of Epilepsy." *BMC Neurology* 18, no. 1: 81. https://doi.org/10.1186/s12883-018-1086-4.

Foudah, A. I., S. Devi, A. Alam, M. A. Salkini, and S. A. Ross. 2023. "Anticholinergic Effect of Resveratrol With Vitamin E on Scopolamine-Induced Alzheimer's Disease in Rats: Mechanistic Approach to Prevent Inflammation." *Frontiers in Pharmacology* 14: 1115721. https://doi.org/10.3389/fphar.2023.1115721.

Gong, C.-X., F. Liu, I. Grundke-Iqbal, and K. Iqbal. 2006. "Impaired Brain Glucose Metabolism Leads to Alzheimer Neurofibrillary Degeneration Through a Decrease in Tau O-GlcNAcylation." *Journal of Alzheimer's Disease* 9, no. 1: 1–12. https://doi.org/10.3233/JAD-2006-9101.

Hamad¹, N., S. E.-s*, S. A.-e, and M. A.-r. 2022. "Molecular Detection and Immune-Profiling of Circulating Very Virulent Infectious Bursal Disease in Broiler Farms in Egypt." *Pakistan Veterinary Journal* 42, no. 3: 316–321.

Hampel, H., M.-M. Mesulam, A. C. Cuello, et al. 2018. "The Cholinergic System in the Pathophysiology and Treatment of Alzheimer's Disease." *Brain* 141, no. 7: 1917–1933. https://doi.org/10.1093/brain/awy132.

Havreng-Théry, C., B. Oquendo, V. Zolnowski-Kolp, et al. 2024. "Cholinesterase Inhibitors and Memantine Are Associated With a Reduced Mortality in Nursing Home Residents With Dementia: A Longitudinal Observational Study." *Alzheimer's Research & Therapy* 16, no. 1: 117. https://doi.org/10.1186/s13195-024-01481-0.

Heimke, M., F. Lenz, U. Rickert, R. Lucius, and F. Cossais. 2022. "Anti-Inflammatory Properties of the SGLT2 Inhibitor Empagliflozin in Activated Primary Microglia." *Cells* 11, no. 19: 3107. https://doi.org/10.3390/cells11193107.

Hierro-Bujalance, C., and M. Garcia-Alloza. 2024. "Empagliflozin Reduces Brain Pathology In Alzheimer's Disease and Type 2 Diabetes." *Neural Regeneration Research* 19, no. 6: 1189–1190. https://doi.org/10.4103/1673-5374.385865.

Hierro-Bujalance, C., C. Infante-Garcia, A. del Marco, et al. 2020. "Empagliflozin Reduces Vascular Damage and Cognitive Impairment in a Mixed Murine Model of Alzheimer's Disease and Type 2 Diabetes." *Alzheimer's Research & Therapy* 12, no. 1: 40. https://doi.org/10.1186/s13195-020-00607-4.

Hirosawa, T., K. Kontani, M. Fukai, et al. 2020. "Different Associations Between Intelligence and Social Cognition in Children With and Without Autism Spectrum Disorders." *PLoS One* 15, no. 8: e0235380. https://doi.org/10.1371/journal.pone.0235380.

Islam, F., S. Shohag, S. Akhter, et al. 2022. "Exposure of Metal Toxicity in Alzheimer's Disease: An Extensive Review." *Frontiers in Pharmacology* 13: 903099. https://doi.org/10.3389/fphar.2022.903099.

Ismaeil, R. A., C. K. Hui, K. A. Affandi, B. Alallam, W. Mohamed, and M. F. Mohd Noor. 2021. "Neuroprotective Effect of Edible Bird's Nest in Chronic Cerebral Hypoperfusion Induced Neurodegeneration in Rats." *Neuroimmunology and Neuroinflammation* 2020: 297–306. https://doi.org/10.20517/2347-8659.2020.63.

Jamshidnejad-Tosaramandani, T., S. Kashanian, M. Babaei, M. H. Al-Sabri, and H. B. Schiöth. 2021. "The Potential Effect of Insulin on AChE and Its Interactions With Rivastigmine In Vitro." *Pharmaceuticals* 14, no. 11: 1136. https://doi.org/10.3390/ph14111136.

Kamatham, P. T., R. Shukla, D. K. Khatri, and L. K. Vora. 2024. "Pathogenesis, Diagnostics, and Therapeutics for Alzheimer's Disease: Breaking the Memory Barrier." *Ageing Research Reviews* 101: 102481. https://doi.org/10.1016/j.arr.2024.102481.

Karthivashan, G., M.-H. Kweon, S.-Y. Park, et al. 2019. "Cognitive-Enhancing and Ameliorative Effects of Acanthoside B in a Scopolamine-Induced Amnesic Mouse Model Through Regulation of Oxidative/Inflammatory/Cholinergic Systems and Activation of the TrkB/CREB/BDNF Pathway." Food and Chemical Toxicology 129: 444–457. https://doi.org/10.1016/j.fct.2019.04.062.

Karthivashan, G., S.-Y. Park, M.-H. Kweon, et al. 2018. "Ameliorative Potential of Desalted Salicornia europaea L. Extract in Multifaceted Alzheimer's-Like Scopolamine-Induced Amnesic Mice Model." *Scientific Reports* 8, no. 1: 7174. https://doi.org/10.1038/s41598-018-25381-0.

Knopman, D. S., H. Amieva, R. C. Petersen, et al. 2021. "Alzheimer Disease." *Nature Reviews Disease Primers* 7, no. 1: 33. https://doi.org/10.1038/s41572-021-00269-y.

Knorz, A. L., and A. Quante. 2022. "Alzheimer's Disease: Efficacy of Mono- and Combination Therapy. A Systematic Review." *Journal of Geriatric Psychiatry and Neurology* 35, no. 4: 475–486. https://doi.org/10.1177/08919887211044746.

Kodam, P., R. Sai Swaroop, S. S. Pradhan, V. Sivaramakrishnan, and R. Vadrevu. 2023. "Integrated Multi-Omics Analysis of Alzheimer's Disease Shows Molecular Signatures Associated With Disease Progression and Potential Therapeutic Targets." *Scientific Reports* 13, no. 1: 3695. https://doi.org/10.1038/s41598-023-30892-6.

Lanteri, R., R. Acquaviva, C. Di Giacomo, et al. 2006. "Heme Oxygenase 1 Expression in Postischemic Reperfusion Liver Damage: Effect of L-Arginine." *Microsurgery* 26, no. 1: 25–32. https://doi.org/10.1002/micr.20206.

Lanzillotta, C., F. Prestia, V. Greco, et al. 2025. "Enhancing Protein O-GlcNAcylation in Down Syndrome Mice Mitigates Memory Dysfunctions Through the Rescue of Mitochondrial Bioenergetics, Stress Responses and Pathological Markers." *Redox Biology* 85: 103769. https://doi.org/10.1016/j.redox.2025.103769.

Lin, B., N. Koibuchi, Y. Hasegawa, et al. 2014. "Glycemic Control With Empagliflozin, a Novel Selective SGLT2 Inhibitor, Ameliorates Cardiovascular Injury and Cognitive Dysfunction in Obese and Type 2 Diabetic Mice." *Cardiovascular Diabetology* 13, no. 1: 148. https://doi.org/10.1186/s12933-014-0148-1.

Liu, F., K. Iqbal, I. Grundke-Iqbal, G. W. Hart, and C.-X. Gong. 2004. "O-GlcNAcylation Regulates Phosphorylation of Tau: A Mechanism Involved in Alzheimer's Disease." *Proceedings of the National Academy of Sciences* 101, no. 29: 10804–10809. https://doi.org/10.1073/pnas.0400348101.

Liu, M., D. Sui, T. Dexheimer, et al. 2020. "Hyperphosphorylation Renders Tau Prone to Aggregate and to Cause Cell Death." *Molecular Neurobiology* 57, no. 11: 4704–4719. https://doi.org/10.1007/s12035-020-02034-w.

Liu, Y., F. Liu, K. Iqbal, I. Grundke-Iqbal, and C.-X. Gong. 2008. "Decreased Glucose Transporters Correlate to Abnormal Hyperphosphorylation of Tau in Alzheimer Disease." *FEBS Letters* 582, no. 2: 359–364. https://doi.org/10.1016/j.febslet.2007.12.035.

Livak, K. J., and T. D. Schmittgen. 2001. "Analysis of Relative Gene Expression Data Using Real-Time Quantitative PCR and the $2-\Delta\Delta$ CT Method." *Methods* 25, no. 4: 402–408. https://doi.org/10.1006/meth. 2001.1262.

Mahaman, Y. A. R., F. Huang, M. T. M. Salissou, et al. 2023. "Ferulic Acid Improves Synaptic Plasticity and Cognitive Impairments by Alleviating the PP2B/DARPP-32/PP1 Axis-Mediated STEP Increase and A β Burden in Alzheimer's Disease." *Neurotherapeutics* 20, no. 4: 1081–1108. https://doi.org/10.1007/s13311-023-01356-6.

Mandour, D.A., M. A. Bendary, and A. E. Alsemeh. 2021. "Histological and Imunohistochemical Alterations of Hippocampus and Prefrontal Cortex in a Rat Model of Alzheimer Like-Disease With a Preferential Role of the Flavonoid "Hesperidin"." *Journal of Molecular Histology* 52, no. 5: 1043–1065. https://doi.org/10.1007/s10735-021-09998-6.

Marucci, G., M. Buccioni, D. D. Ben, C. Lambertucci, R. Volpini, and F. Amenta. 2021. "Efficacy of Acetylcholinesterase Inhibitors in Alzheimer's Disease." *Neuropharmacology* 190: 108352. https://doi.org/10.1016/j.neuropharm.2020.108352.

Mesulam, M., A. Guillozet, P. Shaw, and B. Quinn. 2002. "Widely Spread Butyrylcholinesterase Can Hydrolyze Acetylcholine in the Normal and Alzheimer Brain." *Neurobiology of Disease* 9, no. 1: 88–93. https://doi.org/10.1006/nbdi.2001.0462.

Mishra, E., and M. K. Thakur. 2022. "Alterations in Hippocampal Mitochondrial Dynamics Are Associated With Neurodegeneration and Recognition Memory Decline in Old Male Mice." *Biogerontology* 23, no. 2: 251–271. https://doi.org/10.1007/s10522-022-09960-3.

Moreira, P. I., A. I. Duarte, M. S. Santos, A. C. Rego, and C. R. Oliveira. 2009. "An Integrative View of the Role of Oxidative Stress, Mitochondria and Insulin in Alzheimer's Disease." *Journal of Alzheimer's Disease* 16, no. 4: 741–761. https://doi.org/10.3233/JAD-2009-0972.

Mostafa, D. K., C. A. Ismail, and D. A. Ghareeb. 2016. "Differential Metformin Dose-Dependent Effects on Cognition in Rats: Role of Akt." *Psychopharmacology* 233, no. 13: 2513–2524. https://doi.org/10.1007/s00213-016-4301-2.

Murakami, S., and P. Lacayo. 2022. "Biological and Disease Hallmarks of Alzheimer's Disease Defined by Alzheimer's Disease Genes." *Frontiers in Aging Neuroscience* 14: 996030. https://doi.org/10.3389/fnagi.2022.996030.

Mustroph, J., C. M. Lücht, O. Wagemann, et al. 2019. "Empagliflozin Enhances Human and Murine Cardiomyocyte Glucose Uptake by Increased Expression of GLUT1." *Diabetologia* 62, no. 4: 726–729. https://doi.org/10.1007/s00125-019-4819-z.

Nazam, N., A. Farhana, and S. Shaikh. 2021. "Recent Advances in Alzheimer's Disease in Relation to Cholinesterase Inhibitors and NMDA Receptor Antagonists." In *Autism Spectrum Disorder and Alzheimer's Disease*, 135–151. Springer Nature Singapore. https://doi.org/10.1007/978-981-16-4558-7_8.

Nur Hazaryavuz, A., S. Yildiz, R. K. Kaya, M. E. Cam, and L. Kabasakal. 2022. "Sodium-Glucose Co-Transporter Inhibitor Dapagliflozin Attenuates Cognitive Deficits in Sporadic Alzheimer's Rat Model." *Journal of Research in Pharmacy* 26, no. 2: 298–310. https://doi.org/10.29228/jrp.128.

Ohm, D. T., A. J. Fought, A. Martersteck, et al. 2021. "Accumulation of Neurofibrillary Tangles and Activated Microglia Is Associated With Lower Neuron Densities in the Aphasic Variant of Alzheimer's Disease." *Brain Pathology* 31, no. 1: 189–204. https://doi.org/10.1111/bpa. 12902.

Pan, Y., and J. A. Nicolazzo. 2018. "Impact of Aging, Alzheimer's Disease and Parkinson's Disease on the Blood-Brain Barrier Transport of Therapeutics." *Advanced Drug Delivery Reviews* 135: 62–74. https://doi.org/10.1016/j.addr.2018.04.009.

Pawlos, A., M. Broncel, E. Woźniak, and P. Gorzelak-Pabiś. 2021. "Neuroprotective Effect of SGLT2 Inhibitors." *Molecules* 26, no. 23: 7213. https://doi.org/10.3390/molecules26237213.

Rahman, S. O., B. P. Panda, S. Parvez, et al. 2019. "Neuroprotective Role of Astaxanthin in Hippocampal Insulin Resistance Induced by $A\beta$ Peptides in Animal Model of Alzheimer's Disease." *Biomedicine & Pharmacotherapy = Biomedecine & pharmacotherapie* 110: 47–58. https://doi.org/10.1016/j.biopha.2018.11.043.

Rajamohamedsait, H. B., and E. M. Sigurdsson. 2012. "Histological Staining of Amyloid and Pre-Amyloid Peptides and Proteins in Mouse Tissue." *Methods in Molecular Biology (Clifton, N.J.)* 849: 411–424. https://doi.org/10.1007/978-1-61779-551-0_28.

Ratan, Y., A. Rajput, S. Maleysm, et al. 2023. "An Insight into Cellular and Molecular Mechanisms Underlying the Pathogenesis of Neurodegeneration in Alzheimer's Disease." *Biomedicines* 11, no. 5: 1398. https://doi.org/10.3390/biomedicines11051398.

Rizzo, M. R., I. Di Meo, R. Polito, et al. 2022. "Cognitive Impairment and Type 2 Diabetes Mellitus: Focus of SGLT2 Inhibitors Treatment." *Pharmacological Research* 176: 106062. https://doi.org/10.1016/j.phrs. 2022.106062.

Roy, R. G., P. K. Mandal, and J. C. Maroon. 2023. "Oxidative Stress Occurs Prior to Amyloid A β Plaque Formation and Tau Phosphorylation in Alzheimer's Disease: Role of Glutathione and Metal Ions." *ACS Chemical Neuroscience* 14, no. 17: 2944–2954. https://doi.org/10.1021/acschemneuro.3c00486.

Saad, M. A., A. Rastanawi, and M. F. El-Yamany. 2018. "Alogliptin Abates Memory Injuries of Hepatic Encephalopathy Induced by Acute Paracetamol Intoxication via Switching-Off Autophagy-Related Apoptosis." *Life Sciences* 215: 11–21. https://doi.org/10.1016/j.lfs.2018.10.069.

Safhi, M. M., T. Anwer, G. Khan, R. Siddiqui, S. Moni Sivakumar, and M. F. Alam. 2018. "The Combination of Canagliflozin and Omega-3 Fatty Acid Ameliorates Insulin Resistance and Cardiac Biomarkers *via* Modulation of Inflammatory Cytokines in Type 2 Diabetic Rats." *Korean Journal of Physiology & Pharmacology: Official Journal of the Korean Physiological Society and the Korean Society of Pharmacology* 22, no. 5: 493–501. https://doi.org/10.4196/kjpp.2018.22.5.493.

Samman, W. A., S. M. Selim, H. M. El Fayoumi, N. M. El-Sayed, E. T. Mehanna, and R. M. Hazem. 2023. "Dapagliflozin Ameliorates Cognitive Impairment in Aluminum-Chloride-Induced Alzheimer's Disease via Modulation of AMPK/mTOR, Oxidative Stress and Glucose Metabolism." *Pharmaceuticals* 16, no. 5: 753. https://doi.org/10.3390/ph16050753.

Sa-nguanmoo, P., P. Tanajak, S. Kerdphoo, et al. 2017. "SGLT2-inhibitor and DPP-4 Inhibitor Improve Brain Function via Attenuating Mitochondrial Dysfunction, Insulin Resistance, Inflammation, and Apoptosis in HFD-Induced Obese Rats." *Toxicology and Applied Pharmacology* 333: 43–50. https://doi.org/10.1016/j.taap.2017.08.005.

Shankar, G. M., M. A. Leissring, A. Adame, et al. 2009. "Biochemical and Immunohistochemical Analysis of an Alzheimer's Disease Mouse Model Reveals the Presence of Multiple Cerebral A β Assembly Forms Throughout Life." *Neurobiology of Disease* 36, no. 2: 293–302. https://doi.org/10.1016/j.nbd.2009.07.021.

Sim, A. Y., S. Barua, J. Y. Kim, Y. Lee, and J. E. Lee. 2021. "Role of DPP-4 and SGLT2 Inhibitors Connected to Alzheimer Disease in Type 2 Diabetes Mellitus." *Frontiers in Neuroscience* 15: 708547. https://doi.org/10.3389/fnins.2021.708547.

Sim, A. Y., D. H. Choi, J. Y. Kim, et al. 2023. "SGLT2 and DPP4 Inhibitors Improve Alzheimer's Disease–Like Pathology and Cognitive Function Through Distinct Mechanisms in a T2D–AD Mouse Model." *Biomedicine & Pharmacotherapy = Biomedecine & pharmacotherapie* 168: 115755. https://doi.org/10.1016/j.biopha.2023.115755.

Simanenkova, A. V., O. S. Fuks, N. V. Timkina, et al. 2024. "Highly Selective Sodium-Glucose Co-Transporter Type 2 Inhibitor Empagliflozin as Means of Brain Protection in Conditions of Chronic Brain Dyscirculation." *Problems of Endocrinology* 70, no. 4: 44–56. https://doi.org/10.14341/probl13336.

Snowdon, D. A. 1997. "Aging and Alzheimer's Disease: Lessons From the Nun Study." *Gerontologist* 37, no. 2: 150–156. https://doi.org/10.1093/geront/37.2.150.

Stanciu, G. D., D. C. Ababei, C. Solcan, et al. 2023. "Preclinical Studies of Canagliflozin, a Sodium-Glucose Co-Transporter 2 Inhibitor, and Donepezil Combined Therapy in Alzheimer's Disease." *Pharmaceuticals* 16, no. 11: 1620. https://doi.org/10.3390/ph16111620.

Tang, K. S. 2019. "The Cellular and Molecular Processes Associated With Scopolamine-Induced Memory Deficit: A Model of Alzheimer's Biomarkers." *Life Sciences* 233: 116695. https://doi.org/10.1016/j.lfs. 2019.116695.

Wang, H.-F., J.-T. Yu, S.-W. Tang, et al. 2015. "Efficacy and Safety of Cholinesterase Inhibitors and Memantine in Cognitive Impairment in Parkinson's Disease, Parkinson's Disease Dementia, and Dementia With Lewy Bodies: Systematic Review With Meta-Analysis and Trial Sequential Analysis." *Journal of Neurology, Neurosurgery and Psychiatry* 86, no. 2: 135–143. https://doi.org/10.1136/jnnp-2014-307659.

Xu, M., J. Zheng, T. Hou, et al. 2022. "SGLT2 Inhibition, Choline Metabolites, and Cardiometabolic Diseases: A Mediation Mendelian Randomization Study." *Diabetes Care* 45, no. 11: 2718–2728. https://doi.org/10.2337/dc22-0323.

Yadang, F. S. A., Y. Nguezeye, C. W. Kom, et al. 2020. "Scopolamine-Induced Memory Impairment in Mice: Neuroprotective Effects of *Carissa edulis* (Forssk.) Valh (Apocynaceae) Aqueous Extract." *International Journal of Alzheimer's Disease* 2020: 1–10. https://doi.org/10.1155/2020/6372059.

Yanev, P. G., D. S. Dimitrova, and D. P. Getova-Spassova. 2015. "Effects of Rivastigmine and Memantine Alone and in Combination on Learning and Memory in Rats With Scopolamine-Induced Amnesia." *Open Medicine* 10, no. 1: 338–345. https://doi.org/10.1515/med-2015-0050.

Youn, Y. J., S. Kim, H.-J. Jeong, Y.-M. Ah, and Y. M. Yu. 2024. "Sodium-Glucose cotransporter-2 Inhibitors and Their Potential Role in Dementia Onset and Cognitive Function in Patients With Diabetes Mellitus: A Systematic Review and Meta-Analysis." *Frontiers in Neuroendocrinology* 73: 101131. https://doi.org/10.1016/j.yfrne.2024. 101131.

Supporting Information

Additional supporting information can be found online in the Supporting Information section.

Figure S1: Effect of EMPA, RIVA, and their combination on the level of (a) TNF- α , (b) IL-6, (c) IL-10, (d) SOD, (e) CAT, and (f) MDA in the hippocampus of SCO + HMM rats. Figure S2: Effect of RIVA, EMPA, and their combination on SCO+HMM-induced histopathological changes in cerebral cortex. (a,f) NC depicting normally appearing neurons (black arrow), blood capillaries (red curved arrow), and glia cells (black curved arrow). SCO+HMM group depicting widespread neuronal degeneration with shrunken deeply acidophilic cytoplasm and pyknotic nuclei (yellow arrow), neuronal necrosis (black arrowhead) as well as congestion of meningeal (yellow asterisk) and cerebrocortical blood vessels (black asterisk) and focal meningeal hemorrhages (wavy arrow). (c,h) RIVA-treated group depicting vascular congestion (black asterisk) as well as degenerated (yellow arrow) and necrotic neurons (black arrowhead). (d,i) EMPA-treated group depicting slight dilatation of cortical blood vessels (red arrowhead) and a few degenerated neurons (yellow arrow). (e,j) RIVA+EMPA-treated group depicting marked improvement in the histoarchitecture of the cerebral cortex with normally appearing neurons (black arrow) and only slight vascular congestion (black asterisk). Figure S3: Effect of RIVA, EMPA, and their combination on amyloid plaque deposition in the hippocampus and cerebral cortex. (a,f) NC group, (b,g) SCO+HMM group, (c,h) RIVA treated group, (d,i) EMPA treated group, (e,j) RIVA+EMPA treated group, amyloid plaques (arrow). Congo red stain, Bar = 20µm. (k,l) depicting mean ± SEM of amyloid plaque numbers in both the hippocampus and the cerebral cortex. Table 1: The sets of Real-time PCR primers and annealing temperatures.